Randomized Iterative Methods for Low-Complexity Large-Scale MIMO Detection

Zheng Wang, *Member, IEEE*, Robert M. Gower, Yili Xia, *Member, IEEE*, Lanxin He, and Yongming Huang, *Senior Member, IEEE*

***Abstract*—In this paper, we introduce a randomized iterative method for signal detection in uplink large-scale multiple-input multiple-output (MIMO) systems, which not only achieves a low computational complexity but also enjoys a global and exponentially fast convergence. First of all, by adopting the random sampling into the iterations, the randomized iterative detection algorithm (RIDA) is proposed for large-scale MIMO systems. We show that RIDA converges exponentially fast in terms of mean squared error (MSE). Furthermore, this global convergence *always* holds, and does not depend on the standard requirements such as $N \gg K$, where N and K denote the numbers of antennas at the sides of base station and users. This broadly extends the applications of low-complexity detection in uplink large-scale MIMO systems. Then, based on a new conditional sampling, optimization and enhancements are given to further improve both the convergence and efficiency of RIDA, resulting in the modified randomized iterative detection algorithm (MRIDA). Meanwhile, with respect to MRIDA, further complexity reduction by exploiting the matrix structure is given while its implementation by deep neural networks (DNN) is also presented for a better detection performance.**

***Index Terms*—Massive MIMO detection, low complexity, iterative methods, linear system solver, deep learning.**

I. Introduction

THE large-scale multiple-input multiple-output (MIMO) system has become a promising extension of MIMO in 5 G and beyond 5 G, which boosts the network capacity on a much greater scale without extra bandwidth [1]–[3]. However, the dramatically increased system size also places a pressing challenge on the signal detection in the uplink, where the traditional near-optimal decoding solutions for MIMO detection become prohibitive due to the curse of dimensionality [4], [5]. To this end, a number of advanced detection schemes have been proposed, which aim to achieve the linear detection performance with low computational complexity [6]–[8]. Nevertheless, most of them suffer from some specific convergence requirements, rendering them rather limited in the various scenarios of interest. In fact, compared to the large number of antennas at the base station (BS), the number of antennas of each user equipment (UE) has also improved accordingly. Moreover, with the rapid increment of UE in the last decade, the total number of antennas on the UE side has increased significantly, which makes the environment of wireless communications much more complicated than before [9], [10].

The current methods being deployed to decode the linear system behind large-scale MIMO detection are either based on series expansion or matrix splitting iterative methods. The methods based on series expansion, such as the Neumann series (NS) [11], [12] method are iterative methods that bypass the matrix inversion in the linear detection schemes like zero forcing (ZF) and minimum mean-square error (MMSE). Unfortunately, it has been shown in [13] that the convergence of Neumann series is guaranteed only if the number of receive antennas (denoted by N) is much larger than that of the transmit antennas (denoted by K), i.e., $N \gg K$. Although Newton iteration (NI) was further employed with a better convergence performance than Neumann series, it still suffers from the same requirement for convergence [14], [15]. In fact, such a convergence issue also exists in message passing-based detection algorithms [16], [17]. The matrix splitting methods are also iterative methods, but rather than using a series expansion, are based on splitting the system matrix [18]. However, the convergence of those methods are also restricted by some specific requirements. In Jacobi iteration, the convergence is ensured if the ZF or MMSE filtering matrix $\mathbf{A}$ is strictly diagonally dominant [19]–[21]. As for Richardson iteration, the relaxation factor $0 < \omega < 2/\varrho(\mathbf{A})$ should be well selected for convergence [22]–[24], where $\varrho(\cdot)$ denotes the spectral radius of a matrix. Other low-complexity detection schemes can be found in [25]–[27], but their convergence also depends on the antenna ratio on both sides. If this condition

Manuscript received August 9, 2021; revised January 23, 2022, March 21, 2022, and May 15, 2022; accepted May 27, 2022. Date of publication June 8, 2022; date of current version June 20, 2022. The associate editor coordinating the review of this manuscript and approving it for publication was Dr. An Liu. This work was supported in part by the National Natural Science Foundation of China under Grants 61801216, 61771124, and 61720106003, in part by the Natural Science Foundation of Jiangsu Province under Grant BK20180420, in part by the State Key Laboratory of Integrated Services Networks Xidian University under Grant ISN21-31, in part by the Zhi Shan Young Scholar Program of Southeast University, and in part by the Fundamental Research Funds for the Central Universities under Grant 2242022k30002. *(Corresponding author: Zheng Wang.)*

Zheng Wang is with the School of Information Science and Engineering, Southeast University, Nanjing 210096, China, and also with the State Key Laboratory of Integrated Services Networks, Xidian University, Xian 710071, China (e-mail: z.wang@ieee.org).

Yili Xia and Yongming Huang are with the School of Information Science and Engineering, Southeast University, Nanjing 210096, China (e-mail: yili_xia@seu.edu.cn; huangym@seu.edu.cn).

Lanxin He is with the College of Electronic and Information Engineering, Nanjing University of Aeronautics and Astronautics, Nanjing 210000, China (e-mail: lanxin_he@nuaa.edu.cn).

Robert M. Gower is with the Center for Computational Mathematics, Flatiron Institute and Simons Foundation, New York, NY 10010 USA (e-mail: rgower@flatironinstitute.org).

Digital Object Identifier 10.1109/TSP.2022.3180552

of the ratio of antennas is not met, the performance of these aforementioned detection schemes can be severely degraded or fail to converge.

Recently, sampling turns out to be a powerful strategy for solving decoding problems [28], [29]. In particular, the traditional detection problem can be cast as an equivalent sampling problem [30]–[32]. By doing this, the optimal detection solution can be encountered by sampling from a multi-dimensional discrete Gaussian distribution since it naturally entails the largest sampling probability. By adjusting the standard deviation of the Gaussian distribution, more decoding gains can be achieved with a larger sampling probability of the optimal solution [33]. However, decoding by sampling heavily relies on how to successfully sample from the target discrete Gaussian distribution [34], [35], and this is rather difficult in contrast to the case of sampling from the continuous Gaussian density. Therefore, to effectively exploit the potential behind the randomness, a number of sampling decoding schemes have been proposed, which either perform the sampling over a Gaussian-like distribution [28], [36] or build the Markov chain to realize the random sampling according to Markov chain Monte Carlo (MCMC) methods [37]–[39].

In this paper, in order to achieve a low-complexity signal detection in various cases of interest, we introduce the concept of sampling into the iterative detection methods, where the global and exponential convergence can be achieved. We firstly introduce the randomized iterative detection algorithm (RIDA) for uplink large-scale MIMO systems, which is based on the general sketch-and-project scheme for solving linear systems [40]. By leveraging the convergence theory, we show that RIDA always converges exponentially fast for $N \geq K$. In other words, the randomness in the RIDA method has afforded us a convergence theory that no longer depends on the ratio of antenna. More specifically, its convergence rate for uplink signal detection in large-scale MIMO systems is derived. We then go a step further and introduce the use of conditional sampling and multi-step conditional sampling, which allows us to further speed up the convergence of RIDA. Based on the optimization and enhancement, the modified randomized iterative detection algorithm (MRIDA) is proposed, and an effective complexity reduction solution is given. Moreover, the extension of the proposed MRIDA by deep neural networks (DNN) is also presented, where a better detection performance can be achieved. Compared to the existing iterative detection schemes, the merits of the proposed randomized iterative methods are threefold: low complexity cost, global and fast convergence performance. Overall, our work provides a novel framework for the uplink signal detection of large-scale MIMO systems, where considerable detection gain in terms of both performance and complexity can be explored.

The rest of this paper is organized as follows. Section II briefly introduces the traditional linear detection for uplink large-scale MIMO systems and reviews the low complexity detection schemes by polynomial expansion and iterative method. In Section III, the proposed RIDA is described and its convergence analysis is given to show the global and the exponential convergence. In Section IV, by adopting the conditional sampling into the randomized iteration, further analysis and optimization are carried out. In Section V, MRIDA is proposed to improve the convergence and efficiency, where its complexity reduction and implementation by deep neural networks are also given respectively. After that, simulations of the proposed detection schemes for uplink large-scale MIMO detection are presented in Section VI. Finally, Section VII concludes the paper.

Notation: Matrices and column vectors are denoted by upper and lowercase boldface letters, and the conjugate transpose, inverse, pseudoinverse of a matrix $\mathbf{B}$ by $\mathbf{B}^H, \mathbf{B}^{-1}$, and $\mathbf{B}^\dagger$, respectively. We use $\mathbf{b}_i$ for the ith column of the matrix $\mathbf{B}$, $b_{i,j}$ for the entry in the ith row and jth column of the matrix $\mathbf{B}$. Let $\langle \mathbf{X}, \mathbf{Y} \rangle_{F(\mathbf{W}^{-1})} \triangleq \mathrm{Tr}(\mathbf{X}^H \mathbf{W}^{-1} \mathbf{Y} \mathbf{W}^{-1})$ denote the weighting Frobenius inner product, where $\mathbf{X}, \mathbf{Y} \in \mathbb{C}^{n \times n}$ and $\mathbf{W} \in \mathbb{C}^{n \times n}$ is a symmetric positive definite matrix. Furthermore, let $\|\mathbf{X}\|^2_{F(\mathbf{W}^{-1})} \triangleq \mathrm{Tr}(\mathbf{X}^H \mathbf{W}^{-1} \mathbf{X} \mathbf{W}^{-1}) = \|\mathbf{W}^{-\frac{1}{2}} \mathbf{X} \mathbf{W}^{-\frac{1}{2}}\|^2_F$ where $\|\cdot\|_F$ is the standard Frobenius norm with identity matrix $\mathbf{I}$ and $\mathrm{Tr}(\cdot)$ denotes the trace of the matrix. $\Re(\cdot)$ and $\Im(\cdot)$ indicate the real and imaginary components.

II. Preliminary

In this section, the signal detection in uplink large-scale MIMO systems is reviewed, followed by the background of low-complexity iterative detection schemes derived by polynomial expansion and matrix splitting.

A. Linear Uplink Signal Detection

The base station (BS) in large-scale MIMO system we considered is equipped with N antennas, and simultaneously serves different user equipments (UE), where each UE also equips multiple antennas. To make it simple and straightforward, we use K to denote the total number of antennas at UE side ($N \geq K$). Here, we assume the channel matrix to be perfectly known at BS. Let $\mathbf{x}$ denote the $K \times 1$ transmitted signal vector from UEs and $\mathbf{H} \in \mathbb{C}^{N \times K}$ represent the flat Rayleigh fading channel matrix whose entries are independent and identically distributed (i.i.d.) with zero mean and unit variance. Therefore, the $N \times 1$ received signal vector $\mathbf{y} \in \mathbb{C}^N$ at BS can be expressed as

$$\mathbf{y} = \mathbf{H}\mathbf{x} + \mathbf{n}, \tag{1}$$

where $\mathbf{n}$ is an $N \times 1$ additive white Gaussian noise (AWGN) vector whose entries follow $\mathcal{CN}(\mathbf{0}, \sigma^2)$.

Accordingly, given the system model in (1), to recover the transmitted signal vector $\mathbf{x}$ from the received signal vector $\mathbf{y}$, the optimal maximum likelihood (ML) detection computes

$$\widehat{\mathbf{x}}_{\mathrm{ml}} = \underset{\mathbf{x} \in \mathcal{X}^K}{\arg\min} \|\mathbf{H}\mathbf{x} - \mathbf{y}\|^2, \tag{2}$$

which essentially corresponds to an NP-hard problem. Here, the i-th entry of $\mathbf{x}$, denoted as x_i, is a modulation symbol taken independently from the discrete QAM constellation $\mathcal{X}$. Due to the exponentially increased complexity, the ML detection becomes unaffordable with the increment of system dimension. For this reason, the low-complexity linear detection turns out to be an effective alternative for uplink large-scale MIMO systems.

Specifically, with respect to the system model in (2), the traditional linear ZF and MMSE detectors perform the following

estimations

$$\mathbf{x}_{\text{zf}} = (\mathbf{H}^H\mathbf{H})^{-1}\mathbf{H}^H\mathbf{y} \tag{3}$$

and

$$\mathbf{x}_{\text{mmse}} = \left(\mathbf{H}^H\mathbf{H} + \sigma^2\mathbf{I}\right)^{-1}\mathbf{H}^H\mathbf{y} \tag{4}$$

respectively, where the signal decisions $\widehat{\mathbf{x}}_{\text{zf}}$ and $\widehat{\mathbf{x}}_{\text{mmse}}$ are then determined by rounding $\mathbf{x}_{\text{zf}}$ and $\mathbf{x}_{\text{mmse}}$ according to the modulation constellation $\mathcal{X}^K$, namely,

$$\widehat{\mathbf{x}}_{\text{zf}} = \lceil \mathbf{x}_{\text{zf}} \rfloor_{\text{Round}} \in \mathcal{X}^K \text{ and } \widehat{\mathbf{x}}_{\text{mmse}} = \lceil \mathbf{x}_{\text{mmse}} \rfloor_{\text{Round}} \in \mathcal{X}^K. \tag{5}$$

Note that MMSE detector is optimal according to MSE measure if the sources are Gaussian distributed [41], and the MMSE detection in the context is also denoted as LMMSE in some literatures [8].

It has been shown in [41] that the optimal maximal likelihood (ML) detection performance can be achieved by ZF and MMSE detection if the number of receive antennas at BS goes to infinity (i.e., $N \to \infty$), thus making linear detections popular in tackling with signal detection in uplink large-scale MIMO systems. However, for large dimensional systems, either MMSE or ZF detection turns out to be prohibitive for hardware implementation due to the matrix inversion with computational complexity $\mathcal{O}(K^3)$. Therefore, a number of low-complexity detection schemes are proposed as an effective alternative.

B. Low Complexity Iterative Detection

The linear MMSE detection shown in (4) can be transferred into an equivalent system model by decoding a linear system as follows

$$\mathbf{A}\mathbf{x} = \mathbf{b}, \tag{6}$$

where $\mathbf{b} = \mathbf{H}^H\mathbf{y} \in \mathbb{C}^K$, the MMSE filtering matrix $\mathbf{A} = \mathbf{G} + \sigma^2\mathbf{I} \in \mathbb{C}^{K\times K}$ is symmetric positive, $\mathbf{G} = \mathbf{H}^H\mathbf{H} \in \mathbb{C}^{K\times K}$ is a Gram matrix and $\mathbf{I}$ is a $K \times K$ identity matrix.

To decode the linear system in (6), Neumann series can be applied to arrive at an approximation of matrix inverse about $\mathbf{A}$ by [11]

$$\mathbf{A}^{-1} = \sum_{k=0}^{\infty}(\mathbf{I} - \mathbf{\Theta}\mathbf{A})^k\mathbf{\Theta}, \tag{7}$$

where Θ is a $K \times K$ diagonal matrix and k denotes the iteration index. However, such an approximation holds only if

$$\lim_{k\to\infty}(\mathbf{I} - \mathbf{\Theta}\mathbf{A})^k = \mathbf{0}, \tag{8}$$

which implies the condition $N \gg K$ should be fulfilled in large-scale MIMO systems [13], [16], [42].

Alternatively, we can solve (6) by splitting $\mathbf{A}$ into $\mathbf{A} = \mathbf{P} + \mathbf{Q}$ (matrix $\mathbf{P} \in \mathbb{C}^{K\times K}$ is nonsingular, $\mathbf{Q} \in \mathbb{C}^{K\times K}$), and iterating according to

$$\mathbf{x}^{(k)} = \mathbf{B}\mathbf{x}^{(k-1)} + \mathbf{f}, \tag{9}$$

where $\mathbf{B} = -\mathbf{P}^{-1}\mathbf{Q} = \mathbf{I} - \mathbf{P}^{-1}\mathbf{A} \in \mathbb{C}^{K\times K}$ is known as the iteration matrix and $\mathbf{f} = \mathbf{P}^{-1}\mathbf{b} \in \mathbb{C}^K$. Similarly, the iterative methods also have to confront the convergence problem by satisfying

$$\lim_{k\to\infty}\mathbf{B}^k = \mathbf{0}. \tag{10}$$

In particular, Newton iteration (NI) has a faster convergence rate than Neumann series in dealing with the linear system in (6). Specifically, it has been pointed out in [14], [15] that the result of Newton iteration after k iterations is the same as the $2^k - 1$ order in Neumann series expansion. However, the iterative detection like Newton iteration still suffers from the same convergence requirement as Neumann series[1].

As for Jacobi and Richardson iterative methods, the iteration matrices are set as $\mathbf{B}_{\text{Jacobi}} = \mathbf{I} - \mathbf{D}^{-1}\mathbf{A}$ (i.e., $\mathbf{P} = \mathbf{D}$) and $\mathbf{B}_{\text{Richardson}} = \mathbf{I} - \omega\mathbf{A}$ (i.e., $\mathbf{P} = \frac{1}{\omega}\mathbf{I}$) respectively, where $\mathbf{D} \in \mathbb{C}^{K\times K}$ is the diagonal component of the matrix $\mathbf{A} \in \mathbb{C}^{K\times K}$ and $\omega > 0$ is known as the relaxation parameter. Typically, in order to guarantee the convergence, the matrix $\mathbf{A}$ in Jacobi iteration should be strictly diagonally dominant (SDD) while the Richardson iteration is convergent if $0 < \omega < \frac{2}{\varrho(\mathbf{A})}$. $\varrho(\mathbf{A})$ is the spectral radius of matrix $\mathbf{A}$. Moreover, for a better detection performance, a damping parameter $\delta \in \mathbb{R}$ is adopted into Jacobi iterations to update its iteration matrix as $\mathbf{B}_{\text{damped Jacobi}} = \mathbf{I} - \delta\mathbf{D}^{-1}\mathbf{A}$. However, it has been shown in [43] that the convergence of damped Jacobi only works with $0 < \delta < 2/\varrho(\mathbf{D}^{-1}\mathbf{A})$. Clearly, both the settings of ω and δ are also related to the specific requirement of $\mathbf{A}$ [21] while both of them should be carefully selected for the iteration convergence.

For a faster convergence rate, the method of successive over-relaxation (SOR) was introduced as [44]

$$(\mathbf{D} + \omega\mathbf{L})\mathbf{x}^{k+1} = [(1-\omega)\mathbf{D} - \omega\mathbf{L}^H]\mathbf{x}^k + \omega\mathbf{b} \tag{11}$$

with $\mathbf{A} = \mathbf{D} + \mathbf{L} + \mathbf{L}^H$, where $\mathbf{D}$, $\mathbf{L}$ and $\mathbf{L}^H$ respectively stand for the diagonal components, the strictly lower triangular components and the strictly upper triangular components of $\mathbf{A}$. Unfortunately, the SOR method can converge only for the relaxation parameter $0 < \omega < 2$. Besides, the traditional conjugate gradient method was also introduced to MIMO detection, which is convergent in the signal detection of large-scale MIMO systems [45]. Nevertheless, considerable convergence gain is still worthy to explore for a better detection performance.

III. Randomized Iterative Detection Algorithm

In this section, by capturing the advantages of random sampling, we introduce the randomized iterative detection algorithm (RIDA) for uplink large-scale MIMO system. More precisely, RIDA can be viewed as an application of the sketch-and-project scheme in the complex-valued large-scale MIMO systems [40], [46].

A. Algorithm Description

To reduce the cost of solving the linear system in (6), we first introduce a *sampling matrix* $\mathbf{S} \in \mathbb{C}^{K\times q}$ where q is typically

[1]The requirements of $N \gg K$ for both Neumann series and Newton iteration are specified as $N/K \geq 5.83$ in [13].

much smaller than K, and multiply the system in (6) by the adjoint of $\mathbf{S}$ giving

$$\mathbf{S}^H\mathbf{A}\mathbf{x} = \mathbf{S}^H\mathbf{b}. \tag{12}$$

If $\mathbf{S}$ is a $K \times K$ (i.e., $q = K$) invertible matrix, left multiplying $\mathbf{S}^H$ on both sides of (12) does not alter the solution. However, when $q < K$, then the above equation is reduced to a smaller dimension than the original one, which becomes much easier to solve. But this dimension reduction comes at the price of introducing the existence of more solutions to (12).

To select a unique solution of (12) we use a projection scheme. For this, let $\mathbf{U} \in \mathbb{C}^{K\times K}$ be a symmetric positive definite weighting matrix and let $\mathbf{V} = \mathbf{U}^{\frac{1}{2}} \in \mathbb{C}^{K\times K}$ be the symmetric invertible square root of $\mathbf{U}$. We can now use $\mathbf{V}$ to determine a unique solution to (12) by projecting our current iterate $\mathbf{x}^k$ onto the solution space of (12), that is

$$\begin{aligned}\mathbf{x}^{(k+1)} &= \arg\min_{\mathbf{x}\in\mathbb{C}^K} \|\mathbf{V}(\mathbf{x}-\mathbf{x}^{(k)})\|^2 \\ &\text{subject to } \mathbf{S}_k^H\mathbf{A}\mathbf{x} = \mathbf{S}_k^H\mathbf{b},\ \mathbf{S}_k \sim \mathcal{D},\end{aligned} \tag{13}$$

where k is the iteration index, $\mathbf{S}_k$ follows a discrete distribution $\mathcal{D}$ with $r > 0$ outcomes, i.e., $\mathbf{S}_k \in \{\mathbf{M}_1, \ldots, \mathbf{M}_r\}$, $\mathbf{M}_i \in \mathbb{C}^{K\times q_i}$, $1 \le i \le r$ is a full column rank matrix with probability

$$p_i \triangleq \mathcal{D}(\mathbf{S}_k = \mathbf{M}_i) > 0 \tag{14}$$

and

$$\sum_{i=1}^{r} p_i = 1. \tag{15}$$

According to (13), at each iteration, one samples a new sampling matrix $\mathbf{S}_k$ from $\mathcal{D}$, and computes the new iterate $\mathbf{x}^{(k+1)}$ by choosing the solution of (6) that is as close as possible to $\mathbf{x}^{(k)}$ under the metric determined by the weighting matrix $\mathbf{U}$. Clearly, the distribution $\mathcal{D}$ and the weighting matrix $\mathbf{U}$ serve as the system parameters, which should be carefully designed to guarantee the convergence of the underlying randomized iteration.

In particular, let us introduce a change of variables $\hat{\mathbf{x}} = \mathbf{V}(\mathbf{x} - \mathbf{x}^{(k)})$ in (13) which after re-arranging gives

$$\begin{aligned}&\arg\min \|\hat{x}\|^2 \\ &\text{subject to } \mathbf{S}_k^H\mathbf{A}\mathbf{V}^{-1}\hat{\mathbf{x}} = \mathbf{S}_k^H\left(\mathbf{b} - \mathbf{A}\mathbf{x}^{(k)}\right),\ \mathbf{S}_k \sim \mathcal{D}.\end{aligned} \tag{16}$$

This is now a standard least-norm problem for which the solution is given by the pseudo-inverse of the the system matrix, that is

$$\hat{\mathbf{x}} = \left(\mathbf{S}_k^H\mathbf{A}\mathbf{V}^{-1}\right)^{\dagger}\mathbf{S}_k^H\left(\mathbf{b} - \mathbf{A}\mathbf{x}^{(k)}\right), \tag{17}$$

where $\mathbf{M}^{\dagger}$ denotes the pseudo-inverse of a matrix $\mathbf{M}$. Now using that $\mathbf{M}^{\dagger} = \mathbf{M}^H(\mathbf{M}\mathbf{M}^H)^{-1}$ for every matrix $\mathbf{M}$ we have

$$\begin{aligned}\hat{\mathbf{x}} &= \mathbf{V}^{-1}\mathbf{A}^H\mathbf{S}_k\left(\mathbf{S}_k^H\mathbf{A}\mathbf{V}^{-1}\mathbf{V}^{-1}\mathbf{A}^H\mathbf{S}_k\right)^{-1}\mathbf{S}_k^H\left(\mathbf{b} - \mathbf{A}\mathbf{x}^{(k)}\right) \\ &= \mathbf{V}^{-1}\mathbf{A}^H\mathbf{S}_k\left(\mathbf{S}_k^H\mathbf{A}\mathbf{U}^{-1}\mathbf{A}^H\mathbf{S}_k\right)^{-1}\mathbf{S}_k^H\left(\mathbf{b} - \mathbf{A}\mathbf{x}^{(k)}\right).\end{aligned}$$

Now switching back to the variable $\mathbf{x}$ using $\mathbf{x} = \mathbf{x}^{(k)} + \mathbf{V}^{-1}\hat{\mathbf{x}}$ yields the following expression

$$\mathbf{x}^{(k+1)} = \mathbf{x}^{(k)} + \mathbf{U}^{-1}\mathbf{A}^H\mathbf{S}_k(\mathbf{S}_k^H\mathbf{A}\mathbf{U}^{-1}\mathbf{A}^H\mathbf{S}_k)^{-1}\mathbf{S}_k^H(\mathbf{b} - \mathbf{A}\mathbf{x}^{(k)}) \tag{18}$$

with $\mathbf{S}_k \sim \mathcal{D}$.

To be more specific, let $\mathbf{x}^*$ denote the desired detection solution in (6), i.e., $\mathbf{x}^* = \mathbf{A}^{-1}\mathbf{b}$, the iteration in (18) could be further expressed in a recurrence way as

$$\mathbf{x}^{(k+1)} - \mathbf{x}^* = (\mathbf{I} - \mathbf{U}^{-1}\mathbf{Z})(\mathbf{x}^{(k)} - \mathbf{x}^*) \tag{19}$$

with symmetric matrix $\mathbf{Z} \in \mathbb{C}^{K\times K}$ defined as

$$\mathbf{Z} \triangleq \mathbf{A}^H\mathbf{S}_k(\mathbf{S}_k^H\mathbf{A}\mathbf{U}^{-1}\mathbf{A}^H\mathbf{S}_k)^{-1}\mathbf{S}_k^H\mathbf{A}. \tag{20}$$

From (19), the approximation of $\mathbf{x}^*$ by $\mathbf{x}^{(k)}$ works iteratively under the introduced randomness contained in $\mathbf{Z}$.

Next, to further simplify the randomized iteration in (18), the following choices with respect to systems parameters $\mathcal{D}$ and $\mathbf{U}$ are made. On one hand, by letting $\mathbf{U} = \mathbf{I}$, the iteration in (18) becomes

$$\mathbf{x}^{(k+1)} = \mathbf{x}^{(k)} + \mathbf{A}^H\mathbf{S}_k(\mathbf{S}_k^H\mathbf{A}\mathbf{A}^H\mathbf{S}_k)^{-1}\mathbf{S}_k^H(\mathbf{b} - \mathbf{A}\mathbf{x}^{(k)}). \tag{21}$$

On the other hand, let $\mathbf{S}_k = \mathbf{I}_{:,q_i's}$, where $\mathbf{I}_{:,q_i's}$ denotes a column concatenation containing q_i columns of $K \times K$ identity matrix $\mathbf{I}$ and the q_i columns are uniform randomly selected from $\{1, \ldots, K\}$. Here, to facilitate the efficient sampling, the indices of the q_i selected multiple columns at each time are fixed within a set $\mathcal{Q}_i$, namely,

$$\mathcal{Q}_i = \{\text{index } 1, \ldots, \text{index } q_i\}, \tag{22}$$

thus forming a block operation in the following, e.g.,

$$\underbrace{\{1,2,5\}}_{\mathcal{Q}_1} \cup \ldots \cup \underbrace{\{4,8,12\}}_{\mathcal{Q}_r} = \{1, \ldots, K\} \tag{23}$$

with $q_1 = \cdots = q_i = 3$ and $r = K/q_i$. More precisely, it is clear to see that sets $\mathcal{Q}_i \cap \mathcal{Q}_j = \emptyset$ and $\sum_{i=1}^{r}\mathcal{Q}_i = K$. In this way, the matrix $\mathbf{I}_{:,q_i's}$ can be denoted by $\mathbf{I}_{:,\mathcal{Q}_i}$. Then, based on it, we have

$$\begin{aligned}\mathbf{x}^{(k+1)} &= \mathbf{x}^{(k)} + \mathbf{A}^H\mathbf{I}_{:,q_i's}(\mathbf{I}_{:,q_i's}^H\mathbf{A}\mathbf{A}^H\mathbf{I}_{:,q_i's})^{-1}\mathbf{I}_{:,q_i's}^H(\mathbf{b} - \mathbf{A}\mathbf{x}^{(k)}) \\ &= \mathbf{x}^{(k)} + \mathbf{A}^H\mathbf{I}_{:,\mathcal{Q}_i}(\mathbf{I}_{:,\mathcal{Q}_i}^H\mathbf{A}\mathbf{A}^H\mathbf{I}_{:,\mathcal{Q}_i})^{-1}\mathbf{I}_{:,\mathcal{Q}_i}^H(\mathbf{b} - \mathbf{A}\mathbf{x}^{(k)}) \\ &= \mathbf{x}^{(k)} + \mathbf{A}_{:,\mathcal{Q}_i}(\mathbf{A}_{\mathcal{Q}_i,:}\mathbf{A}_{:,\mathcal{Q}_i})^{-1}(\mathbf{b}_{\mathcal{Q}_i} - \mathbf{A}_{\mathcal{Q}_i,:}\mathbf{x}^{(k)}) \qquad (24) \\ &= \mathbf{x}^{(k)} + \mathbf{A}_{\mathcal{Q}_i,:}^{\dagger}(\mathbf{b}_{\mathcal{Q}_i} - \mathbf{A}_{\mathcal{Q}_i,:}\mathbf{x}^{(k)}) \qquad (25)\end{aligned}$$

where $\mathbf{A}\mathbf{I}_{:,\mathcal{Q}_i} = \mathbf{A}^H\mathbf{I}_{:,\mathcal{Q}_i} = \mathbf{A}_{:,\mathcal{Q}_i} \in \mathbb{C}^{K\times q_i}$ due to the symmetry of $\mathbf{A}$. We point out that with the setups of $\mathbf{U} = \mathbf{I}$, $\mathbf{S}_k = \mathbf{I}_{:,\mathcal{Q}_i}$ as well as block sampling, the proposed randomized iterations behaves like the randomized block Kaczmarz algorithm [47]. Hence, various solutions can be achieved by the proposed randomized iteration scheme with different choices of $\mathbf{U}$ and $\mathcal{D}$, and considerable potential can be exploited therein.

Consequently, by iterating $\mathbf{x}^{(k)}$ according to (25), $\mathbf{x}^*$ can be approximated asymptotically. We point out that $q_i \ll K$ is recommended to fully make use of the reduced linear system in (12). Nevertheless, a larger size q_i means more components of $\mathbf{x}$ can be updated at the same time within one iteration, which

Algorithm 1: Randomized Iterative Detection Algorithm (RIDA) for Uplink Large-Scale MIMO Systems.

Require: $\mathbf{A} = \mathbf{H}^H\mathbf{H} + \sigma^2\mathbf{I}, \mathbf{b} = \mathbf{H}^H\mathbf{y}, \mathbf{x}^{(0)} = \mathbf{0}, Q$
Ensure: near MMSE detection solution $\widehat{\mathbf{x}}^{(k)}$
1: **for** $k = 0, \ldots, Q-1$ **do**
2: randomly sample q_i column indexes according to (23)
3: update $\mathbf{x}^{(k+1)}$ according to (25)
4: **end for**
5: output $\widehat{\mathbf{x}}^{(k)}$ by rounding $\mathbf{x}^{(k)}$ based on constellation $\mathcal{X}^K$

naturally leads to a better convergence performance. As for the initial choice of $\mathbf{x}^{(0)}$, it can be an arbitrary vector and here we use $\mathbf{x}^{(0)} = \mathbf{0}$ as an alternative. To summarize, the operations of the proposed randomized iterative detection algorithm (RIDA) for uplink large-scale MIMO systems is presented in detail in Algorithm 1.

We now consider the computational complexity of RIDA. For the sake of simplicity, we set $q_i = \ldots = q_r = q$. Typically, regarding to the iteration in (24), the computational complexity of calculating $(\mathbf{A}_{\mathcal{Q}_i,:}\mathbf{A}_{:,\mathcal{Q}_i})^{-1}$ is $q^2K + q^3$; the multiplication of $\mathbf{A}_{:,\mathcal{Q}_i}$ and $(\mathbf{A}_{\mathcal{Q}_i,:}\mathbf{A}_{:,\mathcal{Q}_i})^{-1}$ requires $q^2\,K$ computational complexity; the computational complexity of $(\mathbf{b}_{\mathcal{Q}_i} - \mathbf{A}_{\mathcal{Q}_i,:}\mathbf{x}^{(k)})$ is qK while multiplying it with the former term $\mathbf{A}_{:,\mathcal{Q}_i}(\mathbf{A}_{\mathcal{Q}_i,:}\mathbf{A}_{:,\mathcal{Q}_i})^{-1}$ (i.e., $\mathbf{A}^{\dagger}_{\mathcal{Q}_i,:}$) costs qK. Therefore, when $1 \le q \le \sqrt{K}$, the total computational complexity of RIDA at each iteration is no more than $O(K^2)$.

B. Convergence Analysis

We now investigate the convergence of RIDA in terms of the mean squared error (MSE), i.e., $E[\|\mathbf{V}(\mathbf{x}^{(k)} - \mathbf{x}^*)\|^2]$. For convenience, let $\mathbf{M} = [\mathbf{M}_1, \ldots, \mathbf{M}_r] \in \mathbb{C}^{K \times \sum_{i=1}^r q_i}$ and assume $\mathbf{M}_i^H\mathbf{A}$ has full row rank. We will see that it is straightforward to choose a discrete distribution $\mathcal{D}$ for which this rank assumption holds.

As shown in (18), the randomness is invoked by the random sampling $\mathbf{S}_k \sim \mathcal{D}$, which is further contained by matrix $\mathbf{Z}$ in (19). Therefore, in order to show the convergence of the randomized iteration, we firstly characterize $\mathbf{Z}$ in the form of expectation (i.e. $E[\mathbf{Z}]$).

Specifically, in Rayleigh fading channels of large-scale MIMO systems, since the channel matrix $\mathbf{H}$ is a full-rank matrix, the multiplication $\mathbf{Hw}$ for vector $\mathbf{w} \in \mathbb{C}^K$ equals to $\mathbf{0}$ only when $\mathbf{w}$ is a zero vector. Therefore, it is straightforward to verify that the Gram matrix $\mathbf{G}$ contained in matrix $\mathbf{A}$ is positive definite by

$$\mathbf{w}^H\mathbf{G}\mathbf{w} = \mathbf{w}^H\mathbf{H}^H\mathbf{H}\mathbf{w} = (\mathbf{H}\mathbf{w})^H\mathbf{H}\mathbf{w} > 0, \tag{26}$$

which results in a positive definite matrix $\mathbf{A}$ due to $\mathbf{A} = \mathbf{G} + \sigma^2\mathbf{I}$. Then, based on the positive definite matrix $\mathbf{A}$ and the full row rank matrix $\mathbf{M}_i^H\mathbf{A}$, the expectation of $\mathbf{Z}$ can be proved as symmetric positive definite by

$$\begin{aligned} E[\mathbf{Z}] &= \sum_{i=1}^r p_i \mathbf{A}^H\mathbf{M}_i(\mathbf{M}_i^H\mathbf{A}\mathbf{U}^{-1}\mathbf{A}^H\mathbf{M}_i)^{-1}\mathbf{M}_i^H\mathbf{A} \\ &= \mathbf{A}^H\left(\sum_{i=1}^r \mathbf{M}_i p_i^{\frac{1}{2}}\mathbf{Y}_i^{-\frac{1}{2}}\mathbf{Y}_i^{-\frac{1}{2}}p_i^{\frac{1}{2}}\mathbf{M}_i^H\right)\mathbf{A} \\ &= (\mathbf{A}^H\mathbf{M}\mathbf{J})(\mathbf{J}\mathbf{M}^H\mathbf{A}) \end{aligned} \tag{27}$$

with invertible block diagonal matrix $\mathbf{J} \in \mathbb{C}^{K\times K}$, i.e.,

$$\mathbf{J} = \mathrm{diag}(p_1^{\frac{1}{2}}\mathbf{Y}_1^{-\frac{1}{2}}, \ldots, p_r^{\frac{1}{2}}\mathbf{Y}_r^{-\frac{1}{2}}). \tag{28}$$

and $\mathbf{Y}_i = \mathbf{M}_i^H\mathbf{A}\mathbf{U}^{-1}\mathbf{A}^H\mathbf{M}_i$.

According to the symmetric positive definite matrix $E[\mathbf{Z}]$, the following Theorem shows the global exponential convergence of the proposed randomized iteration for uplink detection in large-scale MIMO systems while the proof closely follows [40]. More specifically, it can be viewed as a complex-valued extension of Theorem 16 in [40] with respect to large-scale MIMO systems, where more details have been added to the proof for a better understanding.

Theorem 1: With respect to the uplink detection in large-scale MIMO systems, let $\mathbf{S}_k$ be randomly sampled from the discrete distribution $\mathcal{D}$, the proposed randomized iteration following (18) converges by

$$E[\|\mathbf{V}(\mathbf{x}^{(k)} - \mathbf{x}^*)\|^2] \le \rho^k\|\mathbf{V}(\mathbf{x}^{(0)} - \mathbf{x}^*)\|^2 \tag{29}$$

with exponential convergence rate

$$\rho = 1 - \lambda_{\min}(\mathbf{U}^{-1}E[\mathbf{Z}]) < 1, \tag{30}$$

where $\lambda_{\min}(\cdot)$ denotes the minimum eigenvalue of a matrix.

Proof: First of all, to concisely state the result, the following definition is made

$$\mathbf{r}_k = \mathbf{x}^{(k)} - \mathbf{x}^*. \tag{31}$$

Using the above and the rule of total expectation we have that

$$E[\|\mathbf{V}(\mathbf{x}^{(k)} - \mathbf{x}^*)\|^2] = E[E[\|\mathbf{V}\mathbf{r}_k\|^2|\mathbf{r}_{k-1}]], \tag{32}$$

where the above equality holds according to the *law of total probability* for expectation (i.e., $E[E[A|B]] = E[A]$).

Then, with respect to the term $\|\mathbf{V}\mathbf{r}_k\|^2$ in the above equation, we have the following derivations

$$\begin{aligned} \|\mathbf{V}\mathbf{r}_k\|^2 &= \mathbf{r}_k^H\mathbf{V}^H\mathbf{V}\mathbf{r}_k \\ &\overset{(a)}{=} \mathbf{r}_{k-1}^H(\mathbf{I} - \mathbf{U}^{-1}\mathbf{Z})^H\mathbf{V}^H\mathbf{V}(\mathbf{I} - \mathbf{U}^{-1}\mathbf{Z})\mathbf{r}_{k-1} \\ &= \mathbf{r}_{k-1}^H(\mathbf{V}\mathbf{I} - \mathbf{V}\mathbf{U}^{-1}\mathbf{Z})^H(\mathbf{V}\mathbf{I} - \mathbf{V}\mathbf{U}^{-1}\mathbf{Z})\mathbf{r}_{k-1} \\ &\overset{(b)}{=} \mathbf{r}_{k-1}^H(\mathbf{U}^H - \mathbf{U}^H\mathbf{U}^{-1}\mathbf{Z} - (\mathbf{U}^H\mathbf{U}^{-1}\mathbf{Z})^H + \mathbf{Z}^H\mathbf{U}^{-H}\mathbf{U}^H\mathbf{U}^{-1}\mathbf{Z})\mathbf{r}_{k-1} \\ &\overset{(c)}{=} \mathbf{r}_{k-1}^H(\mathbf{U} - \mathbf{Z} - \mathbf{Z}^H + \mathbf{Z}^H\mathbf{U}^{-1}\mathbf{Z})\mathbf{r}_{k-1} \\ &\overset{(d)}{=} \mathbf{r}_{k-1}^H(\mathbf{U} - 2\mathbf{Z} + \mathbf{Z}^H\mathbf{U}^{-1}\mathbf{Z})\mathbf{r}_{k-1} \\ &\overset{(e)}{=} \mathbf{r}_{k-1}^H(\mathbf{U} - \mathbf{Z})\mathbf{r}_{k-1}. \end{aligned} \tag{33}$$

Here, equality (a) comes from (19) as

$$\mathbf{r}_k = \mathbf{x}^{(k)} - \mathbf{x}^* = (\mathbf{I} - \mathbf{U}^{-1}\mathbf{Z})(\mathbf{x}^{(k)} - \mathbf{x}^*) = (\mathbf{I} - \mathbf{U}^{-1}\mathbf{Z})\mathbf{r}_{k-1}, \tag{34}$$

equality (b) relies on $\mathbf{V}\mathbf{V} = \mathbf{V}\mathbf{V}^H = \mathbf{V}^H\mathbf{V} = \mathbf{U}$ since $\mathbf{V} = \mathbf{U}^{\frac{1}{2}}$ is a symmetric positive definite matrix, equalities (c) and

(d) hold due to the symmetry of matrices $\mathbf{U}$ and $\mathbf{Z}$. Besides, equality (e) comes from the fact that $\mathbf{Z}^H\mathbf{U}^{-1}\mathbf{Z} = \mathbf{Z}$ due to

$$\begin{aligned}&\mathbf{A}^H\mathbf{S}_k(\mathbf{S}_k^H\mathbf{A}\mathbf{U}^{-1}\mathbf{A}^H\mathbf{S}_k)^{-H}\mathbf{S}_k^H\mathbf{A}\mathbf{U}^{-1}\mathbf{A}^H\mathbf{S}_k\\&\quad\times(\mathbf{S}_k^H\mathbf{A}\mathbf{U}^{-1}\mathbf{A}^H\mathbf{S}_k)^{-1}\mathbf{S}_k^H\mathbf{A}\\&=\mathbf{A}^H\mathbf{S}_k(\mathbf{S}_k^H\mathbf{A}\mathbf{U}^{-1}\mathbf{A}^H\mathbf{S}_k)^{-1}\mathbf{S}_k^H\mathbf{A}\\&=\mathbf{Z},\end{aligned}\tag{35}$$

where the matrix $\mathbf{S}_k^H\mathbf{A}\mathbf{U}^{-1}\mathbf{A}^H\mathbf{S}_k$ is symmetric.

Next, based on (33), it follows that

$$\begin{aligned}E[\|\mathbf{V}\mathbf{r}_k\|^2|\mathbf{r}_{k-1}] &= E[\mathbf{r}_{k-1}^H(\mathbf{U}-\mathbf{Z})\mathbf{r}_{k-1}]\\&= E[\mathbf{r}_{k-1}^H\mathbf{V}^H(\mathbf{I}-\mathbf{V}^{-H}\mathbf{Z}\mathbf{V}^{-1})\mathbf{V}\mathbf{r}_{k-1}]\\&= E[\langle(\mathbf{I}-\mathbf{V}^{-H}\mathbf{Z}\mathbf{V}^{-1})\mathbf{V}\mathbf{r}_{k-1},\mathbf{V}\mathbf{r}_{k-1}\rangle]\\&= \langle(\mathbf{I}-\mathbf{V}^{-H}E[\mathbf{Z}]\mathbf{V}^{-1})\mathbf{V}\mathbf{r}_{k-1},\mathbf{V}\mathbf{r}_{k-1}\rangle\\&\le \|\mathbf{I}-\mathbf{V}^{-H}E[\mathbf{Z}]\mathbf{V}^{-1}\|\cdot\|\mathbf{V}\mathbf{r}_{k-1}\|^2\\&\overset{(f)}{=}\lambda_{\max}(\mathbf{I}-\mathbf{V}^{-H}E[\mathbf{Z}]\mathbf{V}^{-1})\|\mathbf{V}\mathbf{r}_{k-1}\|^2\\&= (1-\lambda_{\min}(\mathbf{V}^{-H}E[\mathbf{Z}]\mathbf{V}^{-1}))\|\mathbf{V}\mathbf{r}_{k-1}\|^2\\&= (1-\lambda_{\min}(\mathbf{U}^{-1}E[\mathbf{Z}]))\|\mathbf{V}\mathbf{r}_{k-1}\|^2\\&= \rho\|\mathbf{V}\mathbf{r}_{k-1}\|^2\end{aligned}\tag{36}$$

where the transfer in (f) from operator norm to spectral radius comes from the symmetry of $\mathbf{I}-\mathbf{V}^{-H}E[\mathbf{Z}]\mathbf{V}^{-1}$ and $\lambda_{\max}(\cdot)$ indicates the maximum eigenvalue of a matrix.

After that, by substituting (36) into (32), we have

$$\begin{aligned}E[\|\mathbf{V}(\mathbf{x}^{(k)}-\mathbf{x}^*)\|^2] &\le \rho E[\|\mathbf{V}(\mathbf{x}^{(k-1)}-\mathbf{x}^*)\|^2]\\&\le\cdots\\&\le \rho^k E[\|\mathbf{V}(\mathbf{x}^{(0)}-\mathbf{x}^*)\|^2]\\&= \rho^k\|\mathbf{V}(\mathbf{x}^{(0)}-\mathbf{x}^*)\|^2\end{aligned}\tag{37}$$

where $\mathbf{x}^{(0)}$ is given at the beginning as an initial setup.

On the other hand, because $E[\mathbf{Z}]$ is a symmetric positive definite matrix in large-scale MIMO systems, all the eigenvalues of it are positive, namely, $\lambda_{\min}(E[\mathbf{Z}]) > 0$. Therefore, it follows

$$\rho = 1-\lambda_{\min}(\mathbf{U}^{-1}E[\mathbf{Z}]) < 1,\tag{38}$$

which completes the proof. ■

According to Theorem 1, the randomized iteration converges exponentially fast to the detection solution $\mathbf{x}^*$ of (6). Most importantly, such an exponential convergence always works by $\rho < 1$ for $N \ge K$, making it well suited to various cases of large-scale MIMO systems with respect to both independent, identically distributed (i.i.d.) and correlated channels. Meanwhile, the requirements about system parameters $\mathbf{U}$ and $\mathcal{D}$ are rather loose to be fulfilled, making RIDA different from those aforementioned iterative detection schemes. Additionally, in order to ensure the approximation error smaller than a given value

$$E[\|\mathbf{V}(\mathbf{x}^{(k)}-\mathbf{x}^*)\|^2] \le \epsilon\|\mathbf{V}(\mathbf{x}^{(0)}-\mathbf{x}^*)\|^2\tag{39}$$

with $0 < \epsilon < 1$, the required number of iterations can be estimated by[2]

$$k \ge \frac{1}{1-\rho}\log\left(\frac{1}{\epsilon}\right),\tag{40}$$

which leads to a tractable randomized iteration. Another point should be paid attention to is the choice of $\mathbf{x}^{(0)}$. From (29), a closer choice of $\mathbf{x}^{(0)}$ to the target solution $\mathbf{x}^*$ would significantly reduce the required number of iterations, which is highly recommended in practice.

IV. Optimization and Enhancement

In this section, by resorting to conditional sampling, the prior knowledge of the previous samplings can be fully utilized, thus enabling a better convergence performance. Meanwhile, such a conditional sampling mechanism can be further upgraded to a pseudorandom iteration for better efficiency.

A. Optimization by Conditional Random Sampling

Although the usage of sampling $\mathbf{S}_k$ from $\mathcal{D}$ provides an effective solution to the problem in (12), it does have a side effect during the convergence. Since the randomness in the sampling is hard to control, the sampling diversity would be impeded if a sampling choice $\mathbf{M}_i$ is sampled repeatedly by $\mathbf{S}_{k-1}$ and $\mathbf{S}_k$. To remove such a risk for a better sampling diversity, we propose to update the sampling probability in (14) as a conditional one, which takes the advantages of the prior knowledge from the last sampling, i.e.,

$$\begin{aligned}\overline{p}_i &\triangleq \mathcal{D}(\mathbf{S}_k=\mathbf{M}_i|\mathbf{S}_{k-1}=\mathbf{M}_j),\ i\ne j\\&= \frac{p_i}{1-p_j},\ i\ne j.\end{aligned}\tag{41}$$

Clearly, according to (41), the last sampling $\mathbf{S}_{k-1}$ is considered at the current sampling, and its sampling choice $\mathbf{M}_j$ is removed from the state space of the current sampling for $\mathbf{S}_k$. By doing this, the aforementioned risk that $\mathbf{S}_{k-1} = \mathbf{S}_k$ is avoided, and the randomized iteration is able to achieve a better convergence.

We now go through the conditional randomized iteration given in (41) to confirm its convergence gain. Specifically, based on $\overline{p}_i$ in (41), the conditional expectation of $\mathbf{Z}$ given the last sampling choice $\mathbf{S}_{k-1} = \mathbf{M}_j$ becomes

$$\begin{aligned}E[\mathbf{Z}|\mathbf{S}_{k-1}] =& \sum_{i=1}^{j-1}\overline{p}_i\mathbf{A}^H\mathbf{M}_i(\mathbf{M}_i^H\mathbf{A}\mathbf{U}^{-1}\mathbf{A}^H\mathbf{M}_i)^{-1}\mathbf{M}_i^H\mathbf{A}\\&+\sum_{i=j+1}^{r}\overline{p}_i\mathbf{A}^H\mathbf{M}_i(\mathbf{M}_i^H\mathbf{A}\mathbf{U}^{-1}\mathbf{A}^H\mathbf{M}_i)^{-1}\mathbf{M}_i^H\mathbf{A}\\=&(\mathbf{A}^H\overline{\mathbf{M}}\overline{\mathbf{J}})(\overline{\mathbf{J}}\overline{\mathbf{M}}^H\mathbf{A})\in\mathbb{C}^{K\times K},\end{aligned}\tag{42}$$

which still turns out to be symmetric definite positive with $\overline{\mathbf{M}} = [\mathbf{M}_1,\ldots,\mathbf{M}_{j-1},\mathbf{M}_{j+1},\ldots,\mathbf{M}_r]$ and $\overline{\mathbf{J}} = \mathrm{diag}(\overline{p}_1^{\frac{1}{2}}(\mathbf{M}_1^H\mathbf{A}\mathbf{U}^{-1}\mathbf{A}^H\mathbf{M}_1)^{-\frac{1}{2}},\ldots,\overline{p}_{j-1}^{\frac{1}{2}}(\mathbf{M}_{j-1}^H\mathbf{A}\mathbf{U}^{-1}\mathbf{A}^H\mathbf{M}_{j-1})^{-\frac{1}{2}},$

[2]The inequality $\ln(1-\delta) < -\delta$ for $0 < \delta < 1$ is applied here.

$\overline{p}_{j+1}^{\frac{1}{2}}(\mathbf{M}_{j+1}^H\mathbf{A}\mathbf{U}^{-1}\mathbf{A}^H\mathbf{M}_{j+1})^{-\frac{1}{2}},\ldots,\overline{p}_r^{\frac{1}{2}}(\mathbf{M}_r^H\mathbf{A}\mathbf{U}^{-1}\mathbf{A}^H\mathbf{M}_r)^{-\frac{1}{2}})$. Therefore, it is straightforward to verify that the convergence of such a conditional randomized iteration holds as well and we can easily arrive at the following Theorem, whose proof is omitted due to simplicity.

Theorem 2: Given the sampling choice $\mathbf{S}_{k-1}=\mathbf{M}_j$, $\mathbf{M}_j\in\{\mathbf{M}_1,\ldots,\mathbf{M}_r\}$, let $\mathbf{S}_k$ be randomly sampled according to the conditional sampling probability $\overline{p}_i$ in (41), then the conditional randomized iteration following (18) converges by

$$E[\|\mathbf{V}(\mathbf{x}^{(k)}-\mathbf{x}^*)\|^2]\le\overline{\rho}\|\mathbf{V}(\mathbf{x}^{(k-1)}-\mathbf{x}^*)\|^2 \tag{43}$$

with exponential convergence rate

$$\overline{\rho}=1-\lambda_{\min}(\mathbf{U}^{-1}E[\mathbf{Z}|\mathbf{S}_{k-1}])<1. \tag{44}$$

Note that the convergence rate $\overline{\rho}$ varies at each iteration given the conditional sample $\mathbf{S}_{k-1}$. Subsequently, with respect to the convergence of the conditional randomized iteration, we have the following result by optimization. Here, the squared *Frobenius norm* is applied to calibrate the norm of a matrix in Euclidean space as

$$\|\mathbf{B}\|_F^2=\sum_i^m\sum_j^n|b_{i,j}|^2=\mathrm{Tr}(\mathbf{B}\mathbf{B}^H). \tag{45}$$

Theorem 3: Given the sampling choice $\mathbf{S}_{k-1}=\mathbf{M}_j$, $\mathbf{M}_j\in\{\mathbf{M}_1,\ldots,\mathbf{M}_r\}$, the convergence rate of the conditional randomized iteration takes the form

$$\overline{\rho}_c=1-\frac{\lambda_{\min}(\overline{\mathbf{M}}^H\mathbf{A}\mathbf{U}^{-1}\mathbf{A}^H\overline{\mathbf{M}})}{\|\mathbf{U}^{-\frac{1}{2}}\mathbf{A}^H\overline{\mathbf{M}}\|_F^2} \tag{46}$$

if the sampling probability $\overline{p}_i$ follows

$$\overline{p}_i=\frac{\mathrm{Tr}(\mathbf{M}_i^H\mathbf{A}\mathbf{U}^{-1}\mathbf{A}^H\mathbf{M}_i)}{\|\mathbf{U}^{-\frac{1}{2}}\mathbf{A}^H\overline{\mathbf{M}}\|_F^2},i\ne j. \tag{47}$$

Proof: First of all, for notational simplicity, let $t_i=\mathrm{Tr}(\mathbf{M}_i^H\mathbf{A}\mathbf{U}^{-1}\mathbf{A}^H\mathbf{M}_i)$ and $y_i=(\mathbf{M}_i^H\mathbf{A}\mathbf{U}^{-1}\mathbf{A}^H\mathbf{M}_i)^{-1}$. Then by simple substitution, we have

$$\overline{\mathbf{J}}^2=\frac{\mathrm{diag}(t_1y_1,\ldots,t_{j-1}y_{j-1},t_{j+1}y_{j+1},\ldots,t_ry_r)}{\|\mathbf{U}^{-\frac{1}{2}}\mathbf{A}^H\overline{\mathbf{M}}\|_F^2}. \tag{48}$$

so that

$$\begin{aligned}\lambda_{\min}(\overline{\mathbf{J}}^2)&=\frac{1}{\|\mathbf{U}^{-\frac{1}{2}}\mathbf{A}^H\overline{\mathbf{M}}\|_F^2}\min_{i\ne j}\left\{\frac{t_i}{\lambda_{\max}(\mathbf{M}_i^H\mathbf{A}\mathbf{U}^{-1}\mathbf{A}^H\mathbf{M}_i)}\right\}\\&\overset{(g)}{\ge}\frac{1}{\|\mathbf{U}^{-\frac{1}{2}}\mathbf{A}^H\overline{\mathbf{M}}\|_F^2},\end{aligned} \tag{49}$$

where (g) holds because the trace of a matrix is the sum of its eigenvalues, namely,

$$\mathrm{Tr}(\mathbf{A})=\sum_i\lambda_i(\mathbf{A})\text{ and }\mathrm{Tr}(\mathbf{A})\ge\lambda_{\max}(\mathbf{A})\ge\lambda_{\min}(\mathbf{A}). \tag{50}$$

Then, based on (49) and (42), the following derivation can be achieved

$$\begin{aligned}\lambda_{\min}(\mathbf{U}^{-1}E[\mathbf{Z}|\mathbf{S}_{k-1}])&=\lambda_{\min}(\mathbf{U}^{-\frac{1}{2}}E[\mathbf{Z}|\mathbf{S}_{k-1}]\mathbf{U}^{-\frac{1}{2}})\\&=\lambda_{\min}(\mathbf{U}^{-\frac{1}{2}}\mathbf{A}^H\overline{\mathbf{M}}\overline{\mathbf{J}}^2\overline{\mathbf{M}}^H\mathbf{A}\mathbf{U}^{-\frac{1}{2}})\\&=\lambda_{\min}(\overline{\mathbf{M}}^H\mathbf{A}\mathbf{U}^{-1}\mathbf{A}^H\overline{\mathbf{M}}\overline{\mathbf{J}}^2)\\&\overset{(g)}{\ge}\lambda_{\min}(\overline{\mathbf{M}}^H\mathbf{A}\mathbf{U}^{-1}\mathbf{A}^H\overline{\mathbf{M}})\lambda_{\min}(\overline{\mathbf{J}}^2)\\&\ge\frac{\lambda_{\min}(\overline{\mathbf{M}}^H\mathbf{A}\mathbf{U}^{-1}\mathbf{A}^H\overline{\mathbf{M}})}{\|\mathbf{U}^{-\frac{1}{2}}\mathbf{A}^H\overline{\mathbf{M}}\|_F^2},\end{aligned} \tag{51}$$

where (g) comes from the fact that $\lambda_{\min}(\mathbf{E}\mathbf{F})\ge\lambda_{\min}(\mathbf{E})\lambda_{\min}(\mathbf{F})$ if matrices $\mathbf{E}\in\mathbb{C}^{K\times K}$, $\mathbf{F}\in\mathbb{C}^{K\times K}$ are positive definite. Considering the system parameter $\mathbf{U}$ is set as symmetric positive definite by default, the matrix multiplication $\overline{\mathbf{M}}^H\mathbf{A}\mathbf{U}^{-1}\mathbf{A}^H\overline{\mathbf{M}}$ is positive definite, and so is the matrix $\overline{\mathbf{J}}^2$.

Finally, by substituting (51) into (43), we can arrive at

$$\begin{aligned}E[\|\mathbf{V}(\mathbf{x}^{(k)}-\mathbf{x}^*)\|^2]\le&\left(1-\frac{\lambda_{\min}(\overline{\mathbf{M}}^H\mathbf{A}\mathbf{U}^{-1}\mathbf{A}^H\overline{\mathbf{M}})}{\|\mathbf{U}^{-\frac{1}{2}}\mathbf{A}^H\overline{\mathbf{M}}\|_F^2}\right)^k\\&\times\|\mathbf{V}(\mathbf{x}^{(0)}-\mathbf{x}^*)\|^2.\end{aligned} \tag{52}$$

Furthermore, it can be further expressed as

$$E[\|\mathbf{V}(\mathbf{x}^{(k)}-\mathbf{x}^*)\|^2]\le\overline{\rho}_c^k\|\mathbf{V}(\mathbf{x}^{(0)}-\mathbf{x}^*)\|^2 \tag{53}$$

with

$$\overline{\rho}_c=1-\frac{\lambda_{\min}(\overline{\mathbf{M}}^H\mathbf{A}\mathbf{U}^{-1}\mathbf{A}^H\overline{\mathbf{M}})}{\|\mathbf{U}^{-\frac{1}{2}}\mathbf{A}^H\overline{\mathbf{M}}\|_F^2}\le\overline{\rho} \tag{54}$$

and the sampling probability setup

$$\overline{p}_i=\frac{\mathrm{Tr}(\mathbf{M}_i^H\mathbf{A}\mathbf{U}^{-1}\mathbf{A}^H\mathbf{M}_i)}{\|\mathbf{U}^{-\frac{1}{2}}\mathbf{A}^H\overline{\mathbf{M}}\|_F^2},\ i\ne j, \tag{55}$$

completing the proof. ■

As shown in (46), the convergence rate $\overline{\rho}_c$ is partially determined by the condition number $\kappa=\frac{\lambda_{\max}(\overline{\mathbf{M}}^H\mathbf{A}\mathbf{U}^{-1}\mathbf{A}^H\overline{\mathbf{M}})}{\lambda_{\min}(\overline{\mathbf{M}}^H\mathbf{A}\mathbf{U}^{-1}\mathbf{A}^H\overline{\mathbf{M}})}$. Moreover, according to Theorem 3, it is preferable to improve the convergence rate $\overline{\rho}_c$ by optimizing the choice of the matrix $\overline{\mathbf{M}}=[\mathbf{M}_1,\ldots,\mathbf{M}_{j-1},\mathbf{M}_{j+1},\ldots,\mathbf{M}_r]$. In particular, the convergence rate $\overline{\rho}_c$ can be lower bounded by

$$\begin{aligned}\overline{\rho}_c&=1-\frac{\lambda_{\min}(\overline{\mathbf{M}}^H\mathbf{A}\mathbf{U}^{-1}\mathbf{A}^H\overline{\mathbf{M}})}{\|\mathbf{U}^{-\frac{1}{2}}\mathbf{A}^H\overline{\mathbf{M}}\|_F^2}\\&=1-\frac{\lambda_{\min}(\overline{\mathbf{M}}^H\mathbf{A}\mathbf{U}^{-1}\mathbf{A}^H\overline{\mathbf{M}})}{\mathrm{Tr}(\overline{\mathbf{M}}^H\mathbf{A}\mathbf{U}^{-1}\mathbf{A}^H\overline{\mathbf{M}})}\\&\ge1-\frac{1}{\sum_{i=1}^{j-1}q_i+\sum_{i=j+1}^{r}q_i},\end{aligned} \tag{56}$$

where the lower bound in (56) is reached if and only if $\overline{\mathbf{M}}^H\mathbf{A}\mathbf{U}^{-1}\mathbf{A}^H\overline{\mathbf{M}}=\mathbf{I}$. On the other hand, as for the original randomized iteration, under the same derivation with $p_i=\mathrm{Tr}(\mathbf{M}_i^H\mathbf{A}\mathbf{W}\mathbf{A}^H\mathbf{M}_i)/\|\mathbf{W}^{\frac{1}{2}}\mathbf{A}^H\mathbf{M}\|_F^2$, its convergence rate ρ can be lower bounded as

$$\rho=1-\frac{\lambda_{\min}(\mathbf{M}^H\mathbf{A}\mathbf{W}\mathbf{A}^H\mathbf{M})}{\mathrm{Tr}(\mathbf{M}^H\mathbf{A}\mathbf{W}\mathbf{A}^H\mathbf{M})}\ge1-\frac{1}{\sum_{i=1}^{r}q_i}, \tag{57}$$

where the lower bound is obtained when $\mathbf{M}^H\mathbf{A}\mathbf{U}^{-1}\mathbf{A}^H\mathbf{M}=\mathbf{I}$. Typically, because of $\sum_{i=1}^{j-1}q_i+\sum_{i=j+1}^{r}q_i\leq\sum_{i=1}^{r}q_i$, we can arrive at the following result.

Corollary 1: According to (56) and (57), the conditional randomized iteration outperforms the randomized iteration due to a smaller convergence lower bound of each iteration.

B. Enhancement by Multi-Step Conditional Sampling

Regarding to the conditional randomized iteration, a straightforward enhancement is to involve more previous samplings being considered, i.e.,

$$\overline{p}_L\triangleq\mathcal{D}(\mathbf{S}_k=\mathbf{M}_i|\mathbf{S}_{k-1},\ldots,\mathbf{S}_{k-L}) \tag{58}$$

where $1\leq L\leq r-1$ denotes the number of steps with $\mathbf{M}_i\notin\{\mathbf{S}_{k-1},\ldots,\mathbf{S}_{k-L}\}$. Intuitively, the introduced conditional randomized iteration can be viewed as a special case of multi-step conditional randomized iteration with $L=1$. It is easy to demonstrate that the exponential convergence of the L-step conditional randomized iteration, and we have the following Corollary, whose proof is omitted because of simplicity.

Corollary 2: Given L-step sampling choices $\mathbf{S}_{k-1},\ldots,\mathbf{S}_{k-L}$, let $\mathbf{S}_k$ be randomly sampled according to the conditional sampling probability $\overline{p}_L$ in (58), the L-step conditional randomized iteration following (18) converges by

$$E[\|\mathbf{V}(\mathbf{x}^{(k)}-\mathbf{x}^*)\|^2]\leq\overline{\rho}_L\|\mathbf{V}(\mathbf{x}^{(k-1)}-\mathbf{x}^*)\|^2 \tag{59}$$

with exponential convergence rate

$$\overline{\rho}_L=1-\lambda_{\min}(\mathbf{U}^{-1}E[\mathbf{Z}|\mathbf{S}_{k-1},\ldots,\mathbf{S}_{k-L}])<1. \tag{60}$$

Meanwhile, following Theorem 3, we can see that under the same optimization, the convergence performance of the L-step conditional randomized iteration gradually improves with the increment of L. This actually motivates us to set $L=r-1$ to further exploit the convergence gain due to

$$\overline{\rho}_{r-1}=1-\frac{\lambda_{\min}(\mathbf{M}_i^H\mathbf{A}\mathbf{U}^{-1}\mathbf{A}^H\mathbf{M}_i)}{\mathrm{Tr}(\mathbf{M}_i^H\mathbf{A}\mathbf{U}^{-1}\mathbf{A}^H\mathbf{M}_i)} \tag{61}$$

$$\geq 1-\frac{1}{q_i}. \tag{62}$$

As can be seen clearly, $\overline{\rho}_{r-1}$ has a smaller convergence lower bound than $\overline{\rho}_1$ in (56), thus resulting in a better convergence performance. Besides the convergence gain, more interestingly, when $L=r-1$, the L-step conditional randomized iteration will gradually turn out to be deterministic in selection of $\mathbf{S}_k$. When $k>r-1$, there is only one sampling option left for $\mathbf{S}_k$ given the $r-1$ previous sampling choices of $\mathbf{S}_{k-1},\ldots,\mathbf{S}_{k-r+1}$. Intuitively, such a pseudorandom sampling or derandomization is the natural result of $(r-1)$-step conditional randomized iteration for the iterations $k\geq r-1$. It not only leads to a better iteration efficiency as the operations of random samplings can be avoided, but also is well suited to the hardware implementation in practice. Hence, based on the multi-step conditional randomized iteration with $L=r-1$, the modified randomized iterative detection algorithm (MRIDA) is proposed in what follows.

V. Modified Randomized Iterative Detection Algorithm

In this section, based on the aforementioned optimization and enhancement, the modified randomized iterative detection algorithm (MRIDA) is proposed. Meanwhile, with respect to MRIDA, complexity reduction and implementation by deep neural networks are also presented.

A. Algorithm Description

According to (62), in order to achieve the convergence lower bound of $\overline{\rho}_{r-1}$ in the L-step conditional randomized iteration, the condition $\mathbf{M}_i^H\mathbf{A}\mathbf{U}^{-1}\mathbf{A}^H\mathbf{M}_i=\mathbf{I}$ given $\mathbf{S}_{k-1},\ldots,\mathbf{S}_{k-L}$ with $\mathbf{M}_i\notin\{\mathbf{S}_{k-1},\ldots,\mathbf{S}_{k-L}\}$ should be satisfied. With respect to it, a straightforward way is to choose $\mathbf{U}=\mathbf{A}$ and

$$\mathbf{M}_i=\mathbf{A}^{-\frac{1}{2}}\mathbf{I}_{:,q_i's}=\mathbf{A}^{-\frac{1}{2}}_{:,q_i's}\in\mathbb{C}^{K\times q_i} \tag{63}$$

respectively. However, this is infeasible since the matrix inverse of $\mathbf{A}$ should be avoided in this work due to the consideration of complexity.

Following the optimization choice in (63), we give an approximation of it as an alternative. Specifically, with respect to the symmetric positive matrix $\mathbf{A}=\mathbf{D}+\mathbf{L}+\mathbf{L}^H$, here we apply the diagonal matrix $\mathbf{D}$ as an approximation of $\mathbf{A}$ and we have

$$\mathbf{M}_i'=\mathbf{D}^{-\frac{1}{2}}\mathbf{I}_{:,q_i's}\in\mathbb{C}^{K\times q_i}, \tag{64}$$

where the accuracy of the approximation improves with the increment of the ratio N/K and vice versa.

Therefore, by applying $\mathbf{M}_i'$ into (61) with $\mathbf{U}=\mathbf{A}$, the proposed MRIDA achieves the convergence rate as

$$\overline{\rho}_{r-1}=1-\frac{\lambda_{\min}(\mathbf{M}_i'^H\mathbf{A}\mathbf{M}_i')}{\mathrm{Tr}(\mathbf{M}_i'^H\mathbf{A}\mathbf{M}_i')}. \tag{65}$$

Clearly, the above convergence rate still obeys the lower bound given in (62).

Nevertheless, it has been shown in simulations that this approximation still works even though $N\gg K$ is not fulfilled, making it a general choice for the conditional randomized iteration. Thanks to the favorable propagation in large-scale MIMO systems when $N\gg K$, the MMSE filter matrix $\mathbf{A}=\mathbf{G}+\sigma^2\mathbf{I}$ becomes diagonally dominant due to $\mathbf{h}_i^H\mathbf{h}_j\to 0$ for $i\neq j$ [48]. Meanwhile, because $\mathbf{A}$ is symmetric positive definite, we can conclude that its inverse matrix $\mathbf{A}^{-1}$ is also diagonally dominant. For this reason, such an approximation is recommended for the cases $N\gg K$.

Consequently, given the $r-1$ previous sampling choices $\mathbf{S}_{k-1},\ldots,\mathbf{S}_{k-r+1}$, the sampling choice $\mathbf{S}_k=\mathbf{M}_i'$ can be efficiently determined, and the randomized iteration in (18) with $\mathbf{U}=\mathbf{A}$ becomes

$$\mathbf{x}^{(k+1)}=\mathbf{x}^{(k)}+\mathbf{M}_i'(\mathbf{M}_i'^H\mathbf{A}\mathbf{M}_i')^{-1}(\mathbf{M}_i'^H\mathbf{b}-\mathbf{M}_i'^H\mathbf{A}\mathbf{x}^{(k)}) \tag{66}$$

with

$$\mathbf{M}_i'\notin\{\mathbf{S}_{k-1},\ldots,\mathbf{S}_{k-r+1}\}. \tag{67}$$

Here, for simplicity, the assumption $r=K/q$ and $q_1=\ldots=q_r=q$ is applied in the proposed MRIDA.

Algorithm 2: Modified Randomized Iterative Detection Algorithm (MRIDA) for Uplink Large-Scale MIMO Systems.

Require: $\mathbf{A} = \mathbf{H}^H\mathbf{H} + \sigma^2\mathbf{I}, \mathbf{b} = \mathbf{H}^H\mathbf{y}, \mathbf{x}^{(0)} = \mathbf{D}^{-1}\mathbf{b}, Q$
Ensure: near MMSE detection solution $\widehat{\mathbf{x}}^{(k)}$
1: compute $\mathbf{M}' = \mathbf{D}^{-H}$
2: **for** $k = 0, \ldots, Q-1$ **do**
3: get $\mathbf{M}_i' \notin \{\mathbf{S}_{k-1}, \ldots, \mathbf{S}_{k-r+1}\}$ by L-conditional sampling
4: update $\mathbf{x}^{(k+1)}$ according to (66)
5: **end for**
6: output $\widehat{\mathbf{x}}^{(k)}$ by rounding $\mathbf{x}^{(k)}$ based on constellation $\mathcal{X}^K$

On the other hand, as can be seen from (43) in Theorem 2 and (59) in Corollary 2, a better choice of $\mathbf{x}^{(0)}$ which is closer to $\mathbf{x}^*$ could effectively shorten the need of iterations, so as to a more efficient randomized iterative detection. To this end, the matrix $\mathbf{D}$ is also employed here to determine the initial choice of $\mathbf{x}^{(0)}$ as

$$\mathbf{x}^{(0)} = \mathbf{D}^{-1}\mathbf{b}. \tag{68}$$

Because $\mathbf{D}$ is a diagonal matrix, the computational complexity of obtaining $\mathbf{x}^{(0)}$ in (68) is low, which only requires K multiplications. To summarize, the operation procedures of the proposed MRIDA for uplink large-scale MIMO systems are outlined in Algorithm 2.

B. Complexity Reduction of MRIDA

With respect to the computational complexity of MRIDA, we can see that the computational complexity of calculating $(\mathbf{M}_i'^H\mathbf{A}\mathbf{M}_i')^{-1}$ in (66) is $q^2K + qK^2 + q^3$; the computational complexity of $\mathbf{M}_i'^H\mathbf{b} - \mathbf{M}_i'^H\mathbf{A}\mathbf{x}^{(k)}$ is $2qK + qK^2$ while multiplying these several terms costs $q^2K + qK$. To summarize, when $1 \le q \le \sqrt{K}$, the total computational complexity of MRIDA at each iteration is no more than $O(K^{2.5})$. However, in what follows we show that the computational complexity of MRIPA is actually much lower than that by well taking the structure of matrix $\mathbf{M}_i'$ into account.

According to (64), it is straightforward to see that the matrix $\mathbf{M}_i' = \mathbf{D}^{-\frac{1}{2}}\mathbf{I}_{:,q_i's} \in \mathbb{C}^{K\times q_i}$ entails a special structure. In particular, we can express the selected matrix $\mathbf{M}_i'^H$ as the following way:

$$\mathbf{M}_i'^H = \begin{bmatrix} 0\cdots 0 & m_{1,(i-1)*q+1} & 0 & \cdots & 0 & 0\cdots 0 \\ \vdots\cdots\vdots & 0 & \ddots & \ddots & \vdots & \vdots\cdots\vdots \\ \vdots\cdots\vdots & \vdots & \ddots & \ddots & 0 & \vdots\cdots\vdots \\ 0\cdots 0 & 0 & \cdots & 0 & m_{q,(i-1)*q+q} & 0\cdots 0 \end{bmatrix}.$$

This means the operations of $\mathbf{M}_i'$ or $\mathbf{M}_i'^H$ are actually executed by the $q \times q$ nonzero submatrix within it. Moreover, it is noticeable that the $q \times q$ nonzero submatrix is built by the diagonal elements, where other elements in it are 0 as well. Obviously, this leads to further complexity reduction so that the computational complexity of MRIDA can be expressed in a much lower way.

Specifically, the computational complexity of computing $(\mathbf{M}_i'^H\mathbf{A}\mathbf{M}_i')^{-1}$ in (66) can be reduced to $qK + q^2 + q^3$; the computational complexity of $\mathbf{M}_i'^H\mathbf{b} - \mathbf{M}_i'^H\mathbf{A}\mathbf{x}^{(k)}$ is $q + 2qK$ and multiplying these several terms costs $q^2 + qK$. Considering the choice of $1 \le q \le \sqrt{K}$, the computational complexity of MRIDA at each iteration is no more than $O(K^{1.5})$, which is much lower than $O(K^2)$ of RIDA. This means MRIDA not only achieves a faster convergence rate than RIDA, but also is much more efficient than RIDA, leading to a better detection trade-off between performance and complexity.

Different from the traditional iterative detection schemes which update all the components of $\mathbf{x}$ at each iteration, according to (66) and (25), only q components of $\mathbf{x}$ are updated at each iteration in MRIDA and RIDA. Therefore, for a fair comparison, K/q times iterations are required to complete a full iteration of $\mathbf{x}$ for MRIDA and RIDA. Considering the choice of $1 \le q \le \sqrt{K}$, this corresponds to computational complexities $O(K^2)$ and $O(K^{2.5})$ respectively, which are still competitive compared to those traditional iterative detections. To be more specific, the computational complexities of various low-complexity detection schemes per iteration are listed in Table I. Note that Neumann series only achieves the low complexity (i.e., $O(K^2)$) when the number of iteration is limited by $k \le 2$.

C. Extension by Deep Neural Network

We now upgrade the proposed MRIDA with deep neural networks (DNN), where a non-linear projection operation by training via deep learning (DL) is designed to improve the detection performance.

In [52], the DetNet for large-scale MIMO detection is proposed. Typically, the traditional gradient descent (GD) method is aided by a trained projection operator via DNN as

$$\mathbf{x}^{(k+1)} = \underbrace{\Pi}_{\text{the projection trained by DNN}}\left[\mathcal{F}_{\text{GD}}(\mathbf{x}^{(k)})\right], \tag{69}$$

thus forming an effective iteration to solve the problem in (2). Here $\Pi[\cdot]$ represents a nonlinear projection operation implemented by DNN and $\mathcal{F}_{\text{GD}}(\cdot)$ stands for a specific iteration of gradient descent. Thanks to the nonlinear projection trained by DNN, a better performance than MMSE detection can be archived by DetNet.

Motivated by DetNet, we now try to introduce such a nonlinear projection trained by DNN into the proposed MRIDA in a similar way. First of all, to adopt with deep neural networks, one has to convert the complex-valued system model in (1) to an equivalent one but with real values,

$$\underline{\mathbf{y}} = \underline{\mathbf{H}}\underline{\mathbf{x}} + \underline{\mathbf{n}}, \tag{70}$$

namely,

$$\begin{bmatrix} \Re\{\mathbf{y}\} \\ \Im\{\mathbf{y}\} \end{bmatrix} = \begin{bmatrix} \Re\{\mathbf{H}\} & -\Im\{\mathbf{H}\} \\ \Im\{\mathbf{H}\} & \Re\{\mathbf{H}\} \end{bmatrix}\begin{bmatrix} \Re\{\mathbf{x}\} \\ \Im\{\mathbf{x}\} \end{bmatrix} + \begin{bmatrix} \Re\{\mathbf{n}\} \\ \Im\{\mathbf{n}\} \end{bmatrix}. \tag{71}$$

Clearly, each entry of $\underline{\mathbf{n}}$ follows $\mathcal{N}(\mathbf{0}, \frac{\sigma^2}{2})$. On the other hand, it is straightforward to verify that the proposed MRIDA can also

TABLE I
COMPUTATIONAL COMPLEXITIES OF VARIOUS LOW-COMPLEXITY DETECTION SCHEMES PER ITERATION

MMSE	NS [11]	Newton [15]	Jacobi [19]	Damped Jacobi [43]	Steepest Descend [49]	Richardson [22]
$O(K^3)$	$O(K^2)$ for $k \leq 2$	$O(K^2)$	$O(K^2)$	$O(K^2)$	$O(K^2)$	$O(K^2)$
GS [25]	SOR [50]	CG [45]	AMP-G [16]	GAIMP [51]	RIDA	MRIDA
$O(K^2)$	$O(K^2)$	$O(K^2)$	$O(NK)$	$O(NK)$	$O(K^{2.5})$	$O(K^2)$

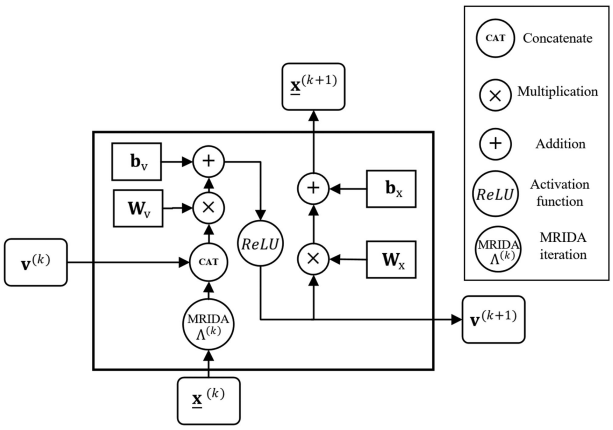

Fig. 1. The structure of MRIDA-Net.

be carried out in the real domain with

$$\underline{\mathbf{x}}^{(k+1)} = \underline{\mathbf{x}}^{(k)} + \mathbf{M}_i'(\mathbf{M}_i'^T\mathbf{A}\mathbf{M}_i')^{-1}(\mathbf{M}_i'^T\mathbf{b} - \mathbf{M}_i'^T\mathbf{A}\underline{\mathbf{x}}^{(k)}), \tag{72}$$

where the related confirmation process is omitted here due to the simplicity.

Then, in the proposed MRIDA-based detection network (MRIDA-Net), a nonlinear projection operation $\Pi(\cdot)$ is incorporated into each iteration as

$$\underline{\mathbf{x}}^{(k+1)} = \Pi\left[\underbrace{\underline{\mathbf{x}}^{(k)} + \mathbf{M}_i'(\mathbf{M}_i'^T\mathbf{A}\mathbf{M}_i')^{-1}(\mathbf{M}_i'^T\mathbf{b} - \mathbf{M}_i'^T\mathbf{A}\underline{\mathbf{x}}^{(k)})}_{\text{operations of MRIDA}}\right]. \tag{73}$$

More specifically, to elaborate this, the following operations are carried out at each iteration

$$\Lambda^{(k)} = \underline{\mathbf{x}}^{(k)} + \mathbf{M}_i'(\mathbf{M}_i'^T\mathbf{A}\mathbf{M}_i')^{-1}(\mathbf{M}_i'^T\mathbf{b} - \mathbf{M}_i'^T\mathbf{A}\underline{\mathbf{x}}^{(k)}), \tag{74}$$

$$\mathbf{v}^{(k+1)} = \mathrm{ReLU}(\mathbf{W}_{\mathrm{v}}[\Lambda^{(k)}, \mathbf{v}^{(k)}] + \mathbf{b}_{\mathrm{v}}), \tag{75}$$

$$\underline{\mathbf{x}}^{(k+1)} = \mathbf{W}_{\mathrm{x}}\mathbf{v}^{(k+1)} + \mathbf{b}_{\mathrm{x}}, \tag{76}$$

where the structure of the proposed MRIDA-Net is illustrated in Fig. 1. Here, $\mathbf{W}_{\mathrm{v}} \in \mathbb{R}^{\alpha K \times (\alpha+2)K}$, $\mathbf{W}_{\mathrm{x}} \in \mathbb{R}^{2K \times \alpha K}$, $\mathbf{b}_{\mathrm{v}} \in \mathbb{R}^{\alpha K}$, $\mathbf{b}_{\mathrm{x}} \in \mathbb{R}^{2K}$ are weights and bias required to quantify during the training phase, $[\cdot]$ is the concatenation, $\mathrm{ReLU}(\cdot)$ is the rectified linear activation function, the hidden vector $\mathbf{v} \in \mathbb{R}^{\alpha K}$ is initialized as zero vector $\mathbf{0}$, and the coefficient $\alpha \geq 2$ is an even integer to adjust the dimension.[3]

[3]The size of the real system $2K \times 2K$ is also considered in α so that α is an even integer.

According to (74), (75)) and (76), the following learnable parameters are introduced into each iteration of MRIDA-Net to build the projection operation $\Pi[\cdot]$

$$\theta = \{\mathbf{W}_{\mathrm{v}}, \mathbf{W}_{\mathrm{x}}, \mathbf{b}_{\mathrm{v}}, \mathbf{b}_{\mathrm{x}}\}. \tag{77}$$

Compared to the gradient descent method in DetNet, the proposed MRIDA achieves a better convergence performance. This means less number of iterations is required by MRIDA, which well suits the parameter-sharing structure of the DNN implementation [53]. Therefore, to enable an efficient training phase, the parameter-sharing structure is employed so that the parameters in set θ are shared among all the projections at each iteration. Meanwhile, we set $\mathbf{W}_{\mathrm{v}}$ and $\mathbf{W}_{\mathrm{x}}$ as sparse matrices, where 70 % of the elements in them are zero-valued. This sparse representation is proposed in [54], and serves as a regularization technique especially beneficial in this high-dimensional case. By doing so, not only the over-fitting issue can be alleviated, but also the total amount of training parameters is further reduced since most of them are set as zero.

Next, the back-propagation algorithm is carried out during the training phase to update θ that minimizes the following weighted loss function

$$f_{\mathrm{Loss}} = \sum_{k=1}^{Q} \log(k+1)\|\underline{\mathbf{x}} - \underline{\mathbf{x}}^{(k)}\|^2. \tag{78}$$

Clearly, the transmitted signal $\underline{\mathbf{x}}$ serves as the training label. Meanwhile, to effectively alleviate the problem of *vanishing gradient* during back-propagation, all the Q outputted $\underline{\mathbf{x}}^{(k)}$ are taken into account by the logarithm weighted structure [52], [55].

As for the complexity of MRIDA-Net, besides the complexity of MRIDA itself (i.e., expressed by (74), the additional computational complexity introduced by the nonlinear projection $\Pi[\cdot]$ consists of calculating the hidden vector $\mathbf{v}^{k+1}$ in (75) and the projected point $\underline{\mathbf{x}}^{k+1}$ in (76), where $2(\alpha+2)^2K^3$ and $2\alpha^2K^3$ multiplications are involved respectively. Therefore, the total computational complexity of MRIDA-Net is $O(K^3)$ while an enhanced detection performance can be achieved under the help of DNN.

VI. SIMULATIONS

In this section, the performance of the proposed RIDA and MRIDA schemes for uplink large-scale MIMO systems are studied by simulations in full detail. For a fair comparison, the full iteration that updates all the components of $\mathbf{x}$ is applied

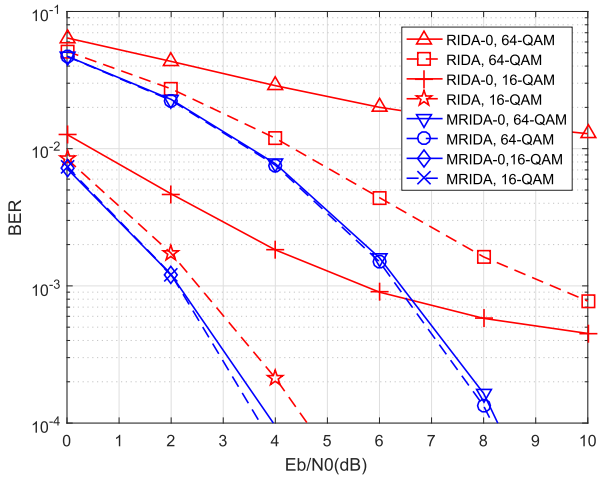

Fig. 2. Bit error rate versus average SNR per bit for the uncoded 16×128 large-scale MIMO system.

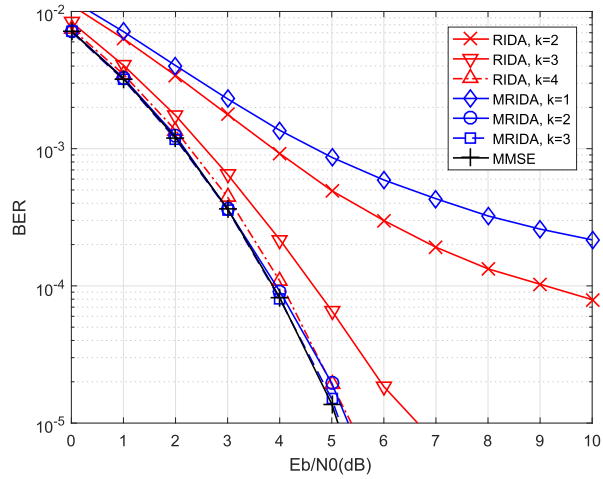

Fig. 3. Bit error rate versus average SNR per bit for the uncoded 16×128 large-scale MIMO system using 16-QAM.

by both RIDA and MRIDA. As for the setup of deep neural networks, the training procedure works on the deep learning (DL) library PyTorch, and MRIDA-Net is trained with Adam Optimizer using a batch size of 20. The learning rate is set as 0.0005 and would decay by 0.97 after each epoch. 50,000 training data are drawn on for each SNR per bit with respect to the training of MRIDA-Net for 32×128 MIMO system with 16-QAM, and 25,000 are utilized under 64×128 scheme with 4-QAM. In our simulations we set $\alpha = 8$ and the overall convergence of the training needs nearly 50 epochs.

In Fig. 2, the initial choices of $\mathbf{x}^{(0)}$ for the proposed randomized iteration schemes are investigated in a 16×128 uncoded large-scale MIMO system. Specifically, two choices of $\mathbf{x}^{(0)} = \mathbf{0}$ and $\mathbf{x}^{(0)} = \mathbf{D}^{-1}\mathbf{b}$ are evaluated respectively while both 16-QAM and 64-QAM are employed to RIDA and MRIDA for a better performance comparison in terms of the bit error rates (BERs). To be more specific, the number of iterations here for RIDA is set as $k = 3$, and the size q in the random selection is set as $q = 4$. Clearly, we can observe that both the detection performance of RIDA and MRIDA with initial settings $\mathbf{x}^{(0)} = \mathbf{D}^{-1}\mathbf{b}$ outperform those with $\mathbf{x}^{(0)} = \mathbf{0}$. This is accordance with our analysis as the choice $\mathbf{x}^{(0)} = \mathbf{D}^{-1}\mathbf{b}$ offers a better approximation to the final detection solution $\mathbf{x}^*$. More precisely, according to Theorem 1, the convergence performance of the proposed randomized iteration scheme is partially determined by the choice of $\mathbf{x}^{(0)}$, so that a reasonable choice of $\mathbf{x}^{(0)}$ naturally leads to a better detection performance. Meanwhile, considering the low complexity of computing $\mathbf{x}^{(0)} = \mathbf{D}^{-1}\mathbf{b}$, it is highly recommended in practice. For this reason, we apply it in the following simulations by default.

In Fig. 3, the performance comparison of the proposed RIDA and MRIDA schemes is illustrated in a 16×128 uncoded large-scale MIMO system with 16-QAM. The detection performance is evaluated in terms of the bit error rates (BERs) while MMSE detection is applied as the baseline. For a fair comparison with other iteration detection schemes, here RIDA and MRIDA update all the components of $\mathbf{x}$ within one full iteration and we set $q = 4$ by default for RIDA and MRIDA

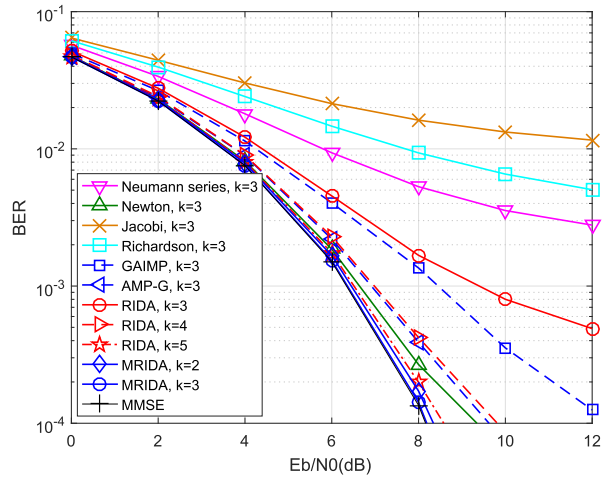

Fig. 4. Bit error rate versus average SNR per bit for the uncoded 16×128 large-scale MIMO system using 64-QAM.

in all the following simulations. For a better illustration of the convergence, the iteration numbers of RIDA and MRIDA are set as $k = 2, 3, 4$ and $k = 1, 2, 3$ respectively. As can be seen clearly, with the increment of iterations, both the detection performance of RIDA and MRIDA improve gradually, thus confirming the convergence of the proposed randomized iteration. We can observe that MRIDA achieves a better convergence performance than RIDA under the same number of iterations. This is in line with the afore-mentioned analysis about the convergence rate and MRIDA does have a better convergence performance by optimization and enhancement. Note that both RIDA with $k = 4$ and MRIDA with $k = 2$ approach the detection performance of MMSE while the MMSE detection performance will be obtained with the increase of k.

The detection performance comparison between RIDA, MRIDA and other conventional iteration schemes are presented in Fig. 4 with respect to a 16×128 uncoded large-scale MIMO system with 64-QAM. Besides MMSE detection scheme, low-complexity detection schemes like the Neumann series in [11],

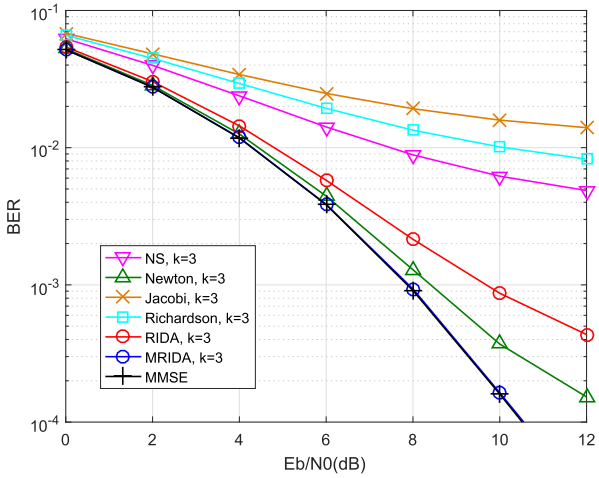

Fig. 5. Bit error rate versus average SNR per bit for the uncoded 16×128 large-scale MIMO system with imperfect CSI using 64-QAM.

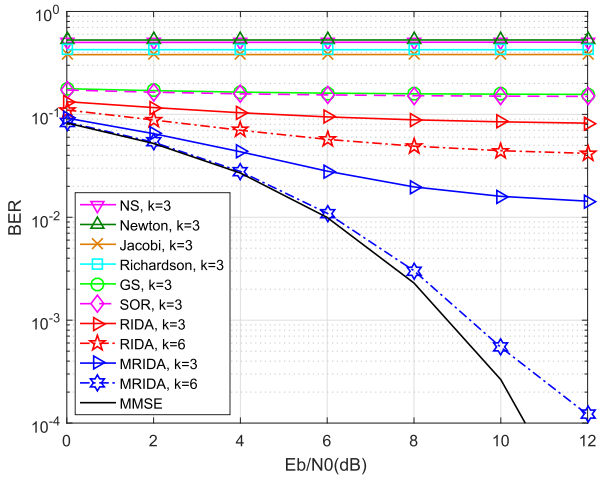

Fig. 6. Bit error rate versus average SNR per bit for the uncoded 16×128 large-scale MIMO using 64-QAM with normalized correlation index $\psi = 0.1$.

Newton iterations in [15], Jacobi iterations in [19], Richardson iterations in [22] with relaxation factor $\omega = 1/(N+K)$[4], the Gaussian approximation of interference message passing (GAIMP) detection in [51] and the approximate message passing with Gaussian approximation (AMP-G) in [16] are also employed. Clearly, under the same iteration number $k = 3$, both RIDA and MRIDA outperform the Neumann series, Jacobi iterations and Richardson iterations, implying a better convergence performance. Meanwhile, with the increment of k, the detection performance of RIDA and MRIDA gradually approach that of MMSE, which verifies the valid convergence performance.

On the other hand, as a counterpart of Fig. 4, Fig. 5 is given to evaluate the detection performance of the proposed RIDA and MRIDA without perfect channel state information (CSI) in a 16×128 uncoded large-scale MIMO systems using 64-QAM. Specifically, $\widehat{\mathbf{H}} = \mathbf{H} + \Delta\mathbf{H}$ stands for the imperfect CSI at the receiver side, where $\Delta\mathbf{H} \sim \mathcal{CN}(\mathbf{0}, \sigma_e^2\mathbf{I}_N)$ denotes the channel estimation errors with $\sigma_e^2 = \frac{K}{n_p \cdot E_p}$ [56]. Here, n_p and E_p indicate the number and the power of pilot symbols respectively, and we set $n_p \cdot E_p = 160$ (i.e., $\sigma_e^2 = 0.1$) for the simulation. Compared to the results of perfect CSI in Fig. 4, the performance of all the detection schemes under imperfect CSI in Fig. 5 degrade accordingly. Clearly, the performance superiority of RIDA and MRIDA can still be confirmed. Note that Newton iterations also achieves a competitive performance in this case. However, it suffers from the convergence condition $N \gg K$ and turns out to be rather limited in various cases of interest in large-scale MIMO systems. To make it clear, the following simulation results are given to further reveal the detection performance when the condition $N \gg K$ is not satisfied.

Besides the independent, identically distributed (i.i.d.) channels, the impact of correlated channels of large-scale MIMO systems is also investigated to reveal the convergence performance of the proposed RIDA and MRIDA schemes. Specifically, following the setups of correlation channels in [57], the correlated channel matrix is set by $\mathbf{R}_{\text{cor}}^{\frac{1}{2}}\mathbf{H}\mathbf{T}_{\text{cor}}^{\frac{1}{2}}$, where $\mathbf{R}_{\text{cor}} \in \mathbb{C}^{N\times N}$ and $\mathbf{T}_{\text{cor}} \in \mathbb{C}^{K\times K}$ denotes the receive correlation matrix and the transmit correlation matrix respectively. Note that the normalized correlation coefficient $1 \geq \psi \geq 0$ is employed to adjust the correlation degree within them. More precisely, a totally uncorrelated scenario corresponds to $\psi = 0$ while a fully correlated scenario implies $\psi = 1$. As can be seen clearly, with $\psi = 0.1$ in Fig. 6, the detection performance of MMSE slightly degrades compared to the i.i.d. case in Fig. 4. Meanwhile, the convergence of the traditional iteration methods like Neumann series, Newton, Jacobi, Richardson suffer from the correlated channels so much, resulting in a terrible detection performance. On the other hand, both the proposed RIDA and MRIDA still work but with slower convergence rates accordingly, which is in line with the derived convergence results. As expected, by increasing the number of iterations, the detection performance of both RIDA and MRIDA improve gradually. The same observations also can be found in the case with $\psi = 0.2$ in Fig. 7, where the channel matrix becomes more correlated. In this condition, the performance of MMSE continues deteriorating.

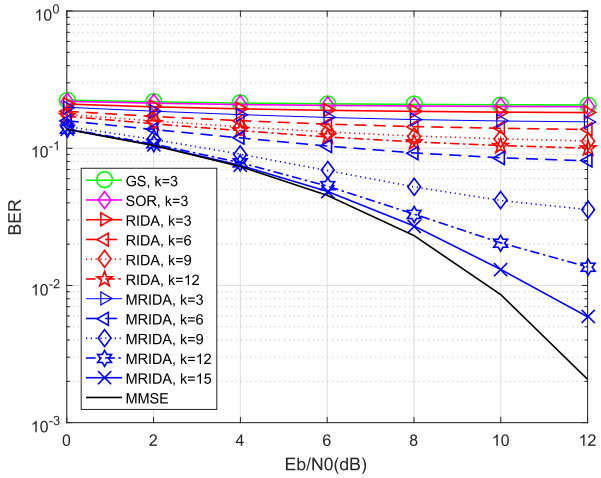

Fig. 7. Bit error rate versus average SNR per bit for the uncoded 16×128 large-scale MIMO using 64-QAM with normalized correlation index $\psi = 0.2$.

[4]This setting of relaxation factor ω is also same with that in [14].

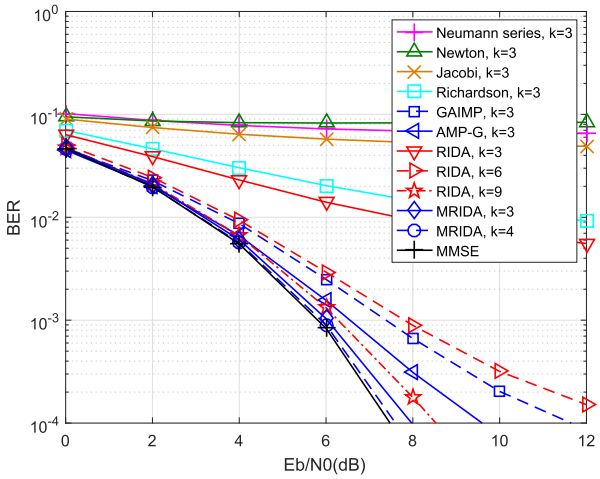

Fig. 8. Bit error rate versus average SNR per bit for the uncoded 32×128 large-scale MIMO system using 16-QAM.

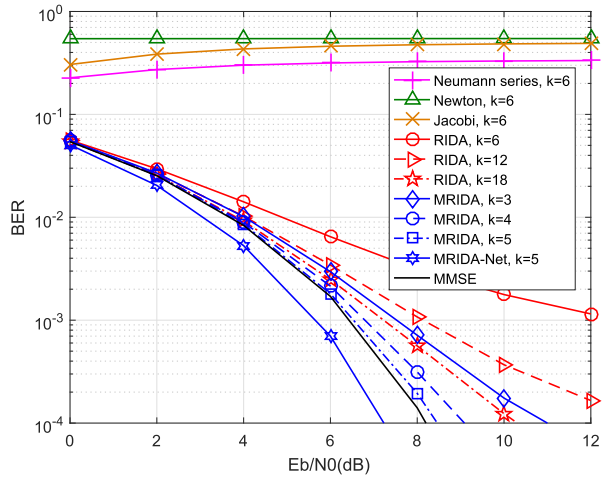

Fig. 9. Bit error rate versus average SNR per bit for the uncoded 64×128 large-scale MIMO system using 4-QAM.

Here, the performance curves of Neumann series, Newton, Jacobi, Richardson are omitted due to their poor performance and we mainly focus on the convergence of RIDA and MRIDA. Clearly, the convergence rates of RIDA and MRIDA become much slower than before. Nevertheless, the convergence of them are still guaranteed but more number of iterations are required to achieve the near MMSE performance. Given the simulation results of $\psi = 0.1$ and $\psi = 0.2$, we can see that the convergence of the proposed RIDA and MRIDA are guaranteed but with slower convergence rates, which is different from the traditional iteration schemes.

In Fig. 8, the bit error rates (BERs) of RIDA and MRIDA with different iteration numbers are illustrated in a 32×128 uncoded large-scale MIMO system with 16-QAM. For a better comparison, the detection schemes like MMSE, Neumann series, Newton iterations, Jacobi iterations and Richardson iterations are added as well. Intuitively, as the convergence requirement $N \gg K$ is not fulfilled in this case, all the convergence performance of Neumann series, Newton iterations and Jacobi iterations are poor, which result in the terrible detection performance accordingly in uplink large-scale MIMO systems. On the contrary, the convergence of both RIDA and MRIDA work well as expected. As demonstrated in Theorem 1, this is because their convergence always hold without suffering from the convergence requirement like $N \gg K$. Therefore, further system gains are exploited by RIDA and MRIDA, which are still at low computational complexity cost. Undoubtedly, with the increase of the iteration number, the detection performance of RIDA and MRIDA improve smoothly while MMSE detection performance can be achieved.

In Fig. 9, we extend the detection performance comparison to a 64×128 uncoded large-scale MIMO system with 4-QAM while the antenna ratio N/K gets smaller. We can observe that the conventional iteration schemes like Neumann series, Newton iterations and Jacobi iterations do not converge any more so that the detection schemes based on them do not work at all. In sharp contrast with them, the proposed RIDA and MRIDA work as usual, and their detection performance gradually improve with

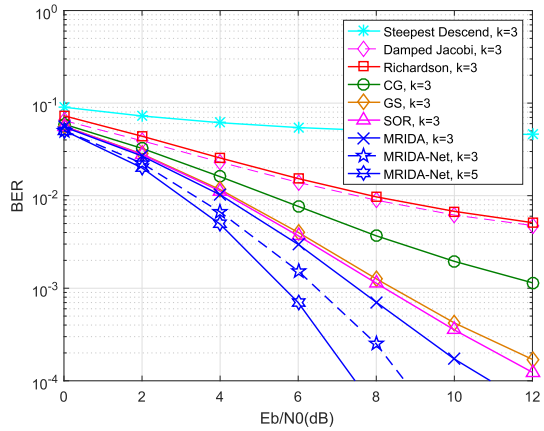

Fig. 10. Bit error rate versus average SNR per bit for the uncoded 64×128 large-scale MIMO system using 4-QAM.

the increment of the number of iterations. It is interesting to see that more iteration numbers are needed compared to the cases 16×128 and 32×128. This is easy to interpret since more correlations over components of $\mathbf{x}$ should be taken into account with the system dimension going up. Clearly, near-MMSE detection performance still can be obtained by the proposed randomized iteration schemes with relatively low computational complexity. On the other hand, based on MRIDA, more detection performance gain can be achieved by the proposed MRIDA-Net. As expected, thank to the nonlinear projection by training via DNN, MRIDA-Net outperforms MMSE considerably.

As a counterpart of Fig. 9, the detection performance comparison between MRIDA and other advanced iterative detection schemes are presented in Fig. 10 with respect to a 64×128 uncoded large-scale MIMO system with 4-QAM. Besides MRIDA, the steepest descent method in [49], the damped Jacobi iterations in [43] with damped parameter $\delta = N/(N + K)$, Richardson iterations in [22], Gauss Seidel iterations in [25], successive over-relaxation (SOR) iterations in [50] with relaxation factor

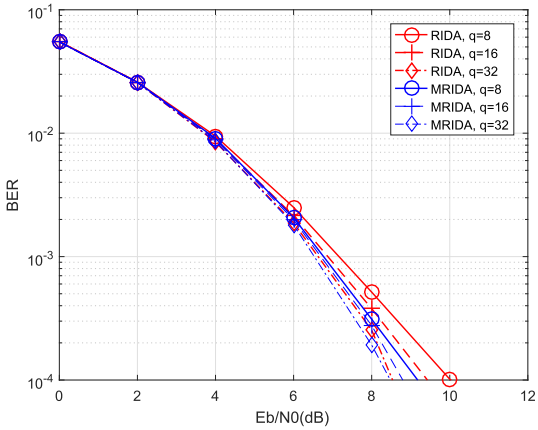

Fig. 11. Bit error rate versus average SNR per bit for the uncoded 64×128 large-scale MIMO system using 4-QAM.

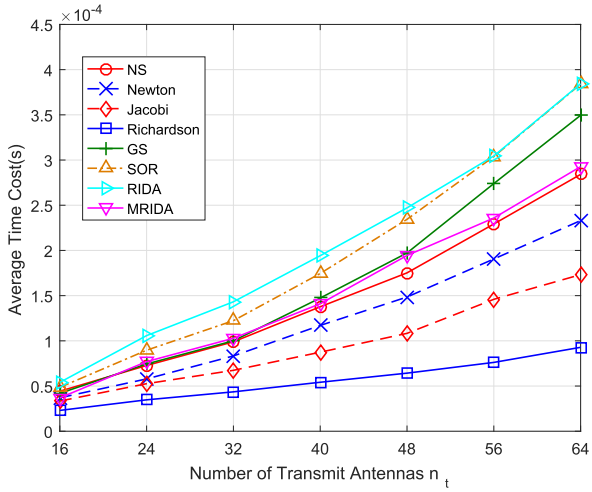

Fig. 12. Complexity comparison in average time cost for the uncoded $K \times 128$ large-scale MIMO system using 16-QAM at SNR per bit $= 8$ dB.

$\omega = \frac{2}{1+\sqrt{1-[\varrho(\mathbf{I}-\mathbf{D}^{-1}\mathbf{A})]^2}}$[5] and conjugate gradient (CG) iterations in [45] are employed. As clearly can be seen, with $k = 3$, all these iterative detection schemes function well without suffering from the requirement $N \gg K$. More specifically, these iterative detection schemes entail different convergence performance while the proposed MRIDA achieves the best convergence, which results in the best detection performance among them for uplink large-scale MIMO systems. Therefore, considerable detection performance gain can be confirmed by adopting the randomness into iterative schemes while the low computational complexity is still maintained. Moreover, under the help of deep neural networks, extra detection performance gain can be obtained by MRIDA-Net.

To investigate the impact of the size q in the proposed randomized iteration schemes, Fig. 11 is presented to illustrate the difference among different choices of q for both RIDA and MRIDA in a 64×128 uncoded large-scale MIMO system with 4-QAM. In particular the choices of $q = 8, 16, 32$ are employed and the numbers of iterations here for RIDA and MRIDA are set as $k = 18$ and $k = 4$ respectively. Clearly, with the increment of size q, the detection performance of both RIDA and MRIDA improve gradually. This is because a larger size q means more components of $\mathbf{x}$ could be updated at one time, so that the correlations between these components can be fully exploited. However, a larger size q also implies more computational cost in the proposed randomized iterative detection schemes so that a reasonable size $1 \leq q \leq \sqrt{K}$ should be selected.

In order to illustrate the computational costs of the proposed RIDA and MRIDA, Fig. 12 is given to show the complexity comparison in average elapsed running times per iteration. In particular, the uncoded MIMO system with $N = 128$ receive anttenas takes 16-QAM at SNR per bit $= 8$dB, and the simulation is conducted by MATLAB R2019a on a single computer, with an Intel Core i7 processor at 2.8 GHz, a RAM of 8 GB and Windows 10 Enterprise Service Pack operating system. As can be seen clearly, the average elapsed running times per iteration of all the detection schemes increase accordingly with the increase of the number of transmit antennas K. Specifically, the average time cost per iteration of MRIDA is lower than that of RIDA, which is competitive compared to GS and SOR iteration schemes. On the other hand, we can observe that Newton iteration, Jacobi iteration and Richardson iteration have smaller average running times than MRIDA and RIDA, but the detection schemes based on them could be poor due to the convergence limitation.

[5]This setting of relaxation factor ω comes from [44].

VII. Conclusion

In this paper, the uplink detection in large-scale MIMO systems is investigated, and two low-complexity iterative detection schemes are proposed to overcome the convergence obstacle in various cases of interest. First of all, by introducing randomness into iteration schemes, the randomized iterative detection algorithm (RIDA) is proposed with computational complexity $O(K^2)$. Then, by analysis, we show that it converges in an exponential way to the target solution, where its convergence rate is also derived. Most importantly, the convergence of the proposed RIDA is always guaranteed for $N \geq K$. This means it does not suffer from the convergence requirements like other iterative detection schemes, thus greatly extending the applications of low-complexity detection schemes in uplink large-scale MIMO systems. After that, by resorting to the conditional sampling, further optimization and enhancement are given, and the modified randomized iterative detection algorithm (MRIDA) is presented for better convergence and efficiency, which leads to a better detection performance in large-scale MIMO systems. Moreover, as for MRIDA, further complexity reduction and implementation by deep neural networks are also given to strengthen its detection efficiency and performance. Therefore, by simply adjusting the number of iterations, flexible detection trade-off between performance and complexity can be achieved by both RIDA and MRIDA in uplink large-scale MIMO systems.

ACKNOWLEDGMENT

The authors would like to thank Prof. Cong Ling (Imperial College London, U.K.) and Prof. Qingjiang Shi (Tongji University, China) for their helpful discussions and insightful suggestions.

REFERENCES

[1] I. Tomkos, D. Klonidis, E. Pikasis, and S. Theodoridis, "Toward the 6G network era: Opportunities and challenges," *IT Professional*, vol. 22, no. 1, pp. 34–38, Jan./Feb. 2020.

[2] F. Tariq, M. R. A. Khandaker, K.-K. Wong, M. A. Imran, M. Bennis, and M. Debbah, "A speculative study on 6G," *IEEE Wireless Commun.*, vol. 27, no. 4, pp. 118–125, Aug. 2020.

[3] W. Saad, M. Bennis, and M. Chen, "A vision of 6G wireless systems: Applications, trends, technologies, and open research problems," *IEEE Netw.*, vol. 34, no. 3, pp. 134–142, May/Jun. 2020.

[4] E. G. Larsson, O. Edfors, F. Tufvesson, and T. L. Marzetta, "Massive MIMO for next generation wireless systems," *IEEE Commun. Mag.*, vol. 52, no. 2, pp. 186–195, Feb. 2014.

[5] D. Tse and P. Viswanath, *Fundamentals of Wireless Communication*. Cambridge, U.K.: Cambridge Univ. Press, 2005.

[6] S. Lyu, J. Wen, J. Weng, and C. Ling, "On low-complexity lattice reduction algorithms for large-scale MIMO detection: The blessing of sequential reduction," *IEEE Trans. Signal Process.*, vol. 68, pp. 257–269, 2020.

[7] K. Pham and K. Lee, "Low-complexity SIC detection algorithms for multiple-input multiple-output systems," *IEEE Trans. Signal Process.*, vol. 63, no. 17, pp. 4625–4633, Sep. 2015.

[8] L. Liu, Y. Chi, C. Yuen, Y. L. Guan, and Y. Li, "Capacity-achieving MIMO-NOMA: Iterative LMMSE detection," *IEEE Trans. Signal Process.*, vol. 67, no. 7, pp. 1758–1773, Apr. 2019.

[9] 3GPP, "User equipment (UE) conformance specification," Tech. Spec., TS 38.521-4 v.15.0.0, May 2019, pp. 1–5.

[10] 3GPP, "Study on scenarios and requirements for next generation access technologies," Tech. Rep., TR 38.913 v.14.3.0, Jun. 2017, pp. 1–41.

[11] F. Rusek *et al.*, "Scaling up MIMO: Opportunities and challenges with very large arrays," *IEEE Signal Process. Mag.*, vol. 30, no. 1, pp. 40–60, Jan. 2013.

[12] M. Wu, B. Yin, G. Wang, C. Dick, J. R. Cavallaro, and C. Studer, "Large-scale MIMO detection for 3GPP LTE: Algorithms and FPGA implementations," *IEEE J. Sel. Topics Signal Process.*, vol. 8, no. 5, pp. 916–929, Oct. 2014.

[13] D. Zhu, B. Li, and P. Liang, "On the matrix inversion approximation based on Neumann series in massive MIMO systems," in *Proc. IEEE Int. Conf. Commun.*, 2015, pp. 1763–1769.

[14] F. Jin, Q. Liu, H. Liu, and P. Wu, "A low complexity signal detection scheme based on improved newton iteration for massive MIMO systems," *IEEE Commun. Lett.*, vol. 23, no. 4, pp. 748–751, Apr. 2019.

[15] C. Tang, C. Liu, L. Yuan, and Z. Xing, "High precision low complexity matrix inversion based on Newton iteration for data detection in the massive MIMO," *IEEE Commun. Lett.*, vol. 20, no. 3, pp. 490–493, Mar. 2016.

[16] S. Wu, L. Kuang, Z. Ni, J. Lu, D. Huang, and Q. Guo, "Low-complexity iterative detection for large-scale multiuser MIMO-OFDM systems using approximate message passing," *IEEE J. Sel. Topics Signal Process.*, vol. 8, no. 5, pp. 902–915, Oct. 2014.

[17] L. Liu, C. Yuen, Y. L. Guan, Y. Li, and Y. Su, "Convergence analysis and assurance for Gaussian message passing iterative detector in massive MU-MIMO systems," *IEEE Trans. Wireless Commun.*, vol. 15, no. 9, pp. 6487–6501, Sep. 2016.

[18] A. Björck, *Numerical Methods for Least Squares Problems*. Philadelphia, PA, USA: SIAM, 1996.

[19] X. Qin, Z. Yan, and G. He, "A near-optimal detection scheme based on joint steepest descent and Jacobi method for uplink massive MIMO systems," *IEEE Commun. Lett.*, vol. 20, no. 2, pp. 276–279, Feb. 2016.

[20] Y. Zhang, A. Yu, X. Tan, Z. Zhang, X. You, and C. Zhang, "Adaptive damped Jacobi detector and architecture for massive MIMO uplink," in *Proc. IEEE Asia Pacific Conf. Circuits Syst.*, 2018, pp. 203–206.

[21] A. Greenbaum, *Iterative Methods for Solving Linear Systems*. Philadelphia, PA, USA: SIAM, 1997.

[22] X. Gao, L. Dai, C. Yuen, and Y. Zhang, "Low-complexity MMSE signal detection based on richardson method for large-scale MIMO systems," in *Proc. IEEE 80th Veh. Technol. Conf.*, 2014, pp. 1–5.

[23] J. Tu, M. Lou, J. Jiang, D. Shu, and G. He, "An efficient massive MIMO detector based on second-order richardson iteration: From algorithm to flexible architecture," *IEEE Trans. Circuits Syst. I: Reg. Papers*, vol. 67, no. 11, pp. 4015–4028, Nov. 2020.

[24] Y. Saad, *Iterative Methods for Sparse Linear Systems*. Philadelphia, PA, USA: SIAM, 1997.

[25] L. Dai, X. Gao, X. Su, S. Han, C.-L. I., and Z. Wang, "Low-complexity soft-output signal detection based on GausscSeidel method for uplink multiuser large-scale MIMO systems," *IEEE Trans. Veh. Technol.*, vol. 64, no. 10, pp. 4839–4845, Oct. 2015.

[26] C. Yang, L. Tang, and Z. Wang, "Enhanced channel hardening-exploiting message passing algorithm for large-scale MIMO detection," in *Proc. IEEE Wireless Commun. Netw. Conf.*, 2021, pp. 1–5.

[27] T. L. Narasimhan and A. Chockalingam, "Channel hardening-exploiting message passing (CHEMP) receiver in large-scale MIMO systems," *IEEE J. Sel. Topics Signal Process.*, vol. 8, no. 5, pp. 847–860, Oct. 2014.

[28] S. Liu, C. Ling, and D. Stehlé, "Decoding by sampling: A randomized lattice algorithm for bounded distance decoding," *IEEE Trans. Inform. Theory*, vol. 57, pp. 5933–5945, Sep. 2011.

[29] P. Klein, "Finding the closest lattice vector when it is unusually close," in *Proc. ACM-SIAM Symp. Discrete Algorithms*, 2000, pp. 937–941.

[30] Z. Wang and C. Ling, "Lattice Gaussian sampling by Markov chain Monte Carlo: Bounded distance decoding and trapdoor sampling," *IEEE Trans. Inf. Theory*, vol. 65, no. 6, pp. 3630–3645, Jun. 2019.

[31] J. Choi, "An MCMC-MIMO detector as a stochastic linear system solver using successive overrelexation," *IEEE Trans. Wireless Commun.*, vol. 15, no. 2, pp. 1445–1455, Feb. 2016.

[32] B. Hassibi, M. Hansen, A. Dimakis, H. Alshamary, and W. Xu, "Optimized Markov chain Monte Carlo for signal detection in MIMO systems: An analysis of the stationary distribution and mixing time," *IEEE Trans. Signal Process.*, vol. 62, no. 17, pp. 4436–4450, Sep. 2014.

[33] Z. Wang and C. Ling, "On the geometric ergodicity of Metropolis-Hastings algorithms for lattice Gaussian sampling," *IEEE Trans. Inf. Theory*, vol. 64, no. 2, pp. 738–751, Feb. 2018.

[34] Z. Wang, "Markov chain Monte Carlo methods for lattice Gaussian sampling: Convergence analysis and enhancement," *IEEE Trans. Commun.*, vol. 67, no. 10, pp. 6711–6724, Oct. 2019.

[35] Z. Wang, Y. Huang, and S. Lyu, "Lattice-reduction-aided Gibbs algorithm for lattice Gaussian sampling: Convergence enhancement and decoding optimization," *IEEE Trans. Signal Process.*, vol. 67, no. 16, pp. 4342–4356, Aug. 2019.

[36] Z. Wang, S. Liu, and C. Ling, "Decoding by sampling - Part II: Derandomization and soft-output decoding," *IEEE Trans. Commun.*, vol. 61, no. 11, pp. 4630–4639, Nov. 2013.

[37] Z. Wang, L. Liu, and C. Ling, "Sliced lattice Gaussian sampling: Convergence improvement and decoding optimization," *IEEE Trans. Commun.*, vol. 69, no. 4, pp. 2599–2612, Apr. 2021.

[38] Z. Wang, S. Lyu, Y. Xia, and Q. Wu, "Expectation propagation-based sampling decoding: Enhancement and optimization," *IEEE Trans. Signal Process.*, vol. 69, pp. 195–209, 2021.

[39] L. Bai, T. Li, J. Liu, Q. Yu, and J. Choi, "Large-scale MIMO detection using MCMC approach with blockwise sampling," *IEEE Trans. Commun.*, vol. 64, no. 9, pp. 3697–3707, Sep. 2016.

[40] R. M. Gower and P. Richtárik, "Randomized iterative methods for linear systems," *SIAM J. Matrix Anal. Appl.*, vol. 36, no. 4, pp. 1660–1690, Dec. 2015.

[41] T. L. Marzetta, "Noncooperative cellular wireless with unlimited numbers of base station antennas," *IEEE Trans. Wireless Commun.*, vol. 9, no. 11, pp. 3590–3600, Nov. 2010.

[42] J.-Y. Jang, W.-S. Lee, J.-H. Ro, Y.-H. You, and H.-K. Song, "Weighted Gauss-Seidel precoder for downlink massive MIMO systems," *Comput., Mater. Continua*, vol. 67, pp. 1729–1745, Jan. 2021.

[43] J. Minango, C. de Almeida, and C. Daniel Altamirano, "Low-complexity MMSE detector for massive MIMO systems based on Damped Jacobi method," in *Proc. IEEE 28th Annu. Int. Symp. Pers., Indoor, Mobile Radio Commun.*, 2017, pp. 1–5.

[44] A. Björck, *Numerical Methods in Matrix Computations*. Berlin, Germany: Springer, 2015.

[45] Y. Hu, Z. Wang, X. Gaol, and J. Ning, "Low-complexity signal detection using CG method for uplink large-scale MIMO systems," in *Proc. IEEE Int. Conf. Commun. Syst.*, 2014, pp. 477–481.

[46] R. M. Gower, "Sketch and project: Randomized iterative methods for linear systems and inverting matrices," 2016, *arXiv:1612.06013*.

[47] T. Strohmer and R. Vershynin, "A randomized Kaczmarz algorithm with exponential convergence," *J. Fourier Anal. Appl.*, vol. 15, no. 2, pp. 262–278, 2009.

[48] Z. Chen and E. Björnson, "Channel hardening and favorable propagation in cell-free massive MIMO with stochastic geometry," *IEEE Trans. Commun.*, vol. 66, no. 11, pp. 5205–5219, Nov. 2018.
[49] Y. Xue, C. Zhang, S. Zhang, Z. Wu, and X. You, "Steepest descent method based soft-output detection for massive MIMO uplink," in *Proc. IEEE Int. Workshop Signal Process. Syst.*, 2016, pp. 273–278.
[50] P. Zhang, L. Liu, G. Peng, and S. Wei, "Large-scale MIMO detection design and FPGA implementations using SOR method," in *Proc. 8th IEEE Int. Conf. Commun. Softw. Netw.*, 2016, pp. 206–210.
[51] P. Som, T. Datta, N. Srinidhi, A. Chockalingam, and B. S. Rajan, "Low-complexity detection in large-dimension MIMO-ISI channels using graphical models," *IEEE J. Sel. Topics Signal Process.*, vol. 5, no. 8, pp. 1497–1511, Dec. 2011.
[52] N. Samuel, T. Diskin, and A. Wiesel, "Learning to detect," *IEEE Trans. Signal Process.*, vol. 67, no. 10, pp. 2554–2564, May 2019.
[53] L. Y. Dawei Dai and H. Wei, "Parameters sharing in residual neural networks," *Neural Process. Lett.*, vol. 51, pp. 1393–1410, Apr. 2020.
[54] S. Ahmad and L. Scheinkman, "How can we be so dense? The benefits of using highly sparse representations," 2019, *arXiv:1903.11257*.
[55] N. Samuel, T. Diskin, and A. Wiesel, "Deep MIMO detection," in *Proc. IEEE 18th Int. Workshop Signal Process. Adv. Wireless Commun.*, 2017, pp. 1–5.
[56] Q. Chen, S. Zhang, S. Xu, and S. Cao, "Efficient MIMO detection with imperfect channel knowledge - A deep learning approach," in *Proc. IEEE Wireless Commun. Netw. Conf.*, 2019, pp. 1–6.
[57] B. Costa, A. Mussi, and T. Ab, "MIMO detectors under correlated channels," *Semina: Ciencias Exatas e Tecnologicas*, vol. 37, no. 1, pp. 3–12, 2016.

Zheng Wang (Member, IEEE) received the B.S. degree in electronic and information engineering from the Nanjing University of Aeronautics and Astronautics, Nanjing, China, in 2009, and the M.S. degree in communications from the University of Manchester, Manchester, U.K., in 2010, and the Ph.D. degree in communication engineering from Imperial College London, London, U.K., in 2015.

Since 2021, he has been an Associate Professor with the School of Information and Engineering, Southeast University, Nanjing, China. From 2015 to 2016, he was a Research Associate with Imperial College London, London, U.K. From 2016 to 2017, he was a Senior Engineer with Radio Access Network R&D division, Huawei Technologies Company. From 2017 to 2020, he was an Associate Professor with the College of Electronic and Information Engineering, Nanjing University of Aeronautics and Astronautics, Nanjing, China. His research interests include massive MIMO systems, machine learning and data analytics over wireless networks, and lattice theory for wireless communications.

Robert M. Gower received the bachelor's and master's degree in applied mathematics from the State University of Campinas, Campinas, Brazil, and the Ph.D. degree in applied mathematics from The University of Edinburgh, Edinburgh, U.K. He designed the current state-of-the-art algorithms for automatically calculating high order derivatives using backpropagation with the State University of Campinas. He is currently a Research Scientist with Flatiron Institute, New York, NY, USA. Before that, he was a Visiting Scientist and Google Brain in 2021 and Facebook AI Research in 2020 New York, and has been an Assistant Professor lcom Paris, Institut Polytechnique since 2017. In his thesis, he introduced the new sketch-and-project methods for solving linear systems.

Yili Xia (Member, IEEE) received the B.Eng. degree in information engineering from Southeast University, Nanjing, China, in 2006, the M.Sc. (with distinction) degree in communications and signal processing from the Department of Electrical and Electronic Engineering, Imperial College London, London, U.K., in 2007, and the Ph.D. degree in adaptive signal processing from Imperial College London, in 2011.

Since 2013, he has been an Associate Professor in signal processing with the School of Information Science and Engineering, Southeast University, Nanjing, China, where he is currently the Deputy Head of the Department of Information and Signal Processing Engineering. His research interests include complex and hyper-complex statistical analysis, detection and estimation, linear and nonlinear adaptive filters, and their applications on communications and power systems. Dr. Xia was the recipient of the Best Student Paper Award at the International Symposium on Neural Networks in 2010 (coauthor), and the Education Innovation Award at the IEEE International Conference on Acoustics, Speech, and Signal Processing in 2019. He is currently an Associate Editor for the IEEE TRANSACTIONS ON SIGNAL PROCESSING.

Lanxin He received the B.S. degree in 2021 from the College of Electronic and Information Engineering, Nanjing University of Aeronautics and Astronautics, Nanjing, China, where she is currently working toward the M.S. degree. Her research interests include machine learning and deep learning applications on uplink signal detection of massive MIMO systems.

Yongming Huang (Senior Member, IEEE) received the B.S. and M.S. degrees from Nanjing University, Nanjing, China, in 2000 and 2003, respectively, and the Ph.D. degree in electrical engineering from Southeast University, Nanjing, China, in 2007.

Since March 2007, he has been a Faculty with the School of Information Science and Engineering, Southeast University, where he is currently a Full Professor. During 2008–2009, he visited the Signal Processing Lab, Royal Institute of Technology, Stockholm, Sweden. He has authored or coauthored more than 200 peer-reviewed papers, and holds more than 80 invention patents. His research interests include intelligent 5G/6G mobile communications and millimeter wave wireless communications. He submitted around 20 technical contributions to IEEE standards, and was awarded a certificate of appreciation for outstanding contribution to the development of IEEE standard 802.11aj. He was an Associate Editor for the IEEE TRANSACTIONS ON SIGNAL PROCESSING and the Guest Editor of the IEEE JOURNAL SELECTED AREAS IN COMMUNICATIONS. He is currently the Editor-at-Large of the IEEE Open Journal of the Communications Society and an Associate Editor for the IEEE WIRELESS COMMUNICATIONS LETTERS.